Developmentally-Inspired Engineering Of An Inductive Biomaterial for Odontogenesis

Developmentally-Inspired Engineering Of An Inductive Biomaterial for Odontogenesis

A dissertation presented

by

Basma Hashmi

to

The School of Engineering and Applied Sciences

in partial fulfillment of the requirements

for the degree of

Doctor of Philosophy

in the subject of

Engineering Sciences

Harvard University
Cambridge, Massachusetts

May 2014

Professor Donald E. Ingber Basma Hashmi

Developmentally-Inspired Engineering Of An Inductive Biomaterial for Odontogenesis

Abstract

Increasing demands for organ transplants and the depleting supply of available organs has heightened the need for alternatives to this growing problem. Tissue engineers strive to regenerate organs in the future; however doing so requires a fundamental understanding of organ development and its key processes. The first chapter of this thesis provides a brief overview of developmentally inspired engineering, specifically in the context of how I approach this challenge in this thesis. The second chapter provides an in depth review of current and past work focused on organ regeneration from a developmentally-inspired perspective, and using tooth formation as a model system. The third chapter describes the design and fabrication of a thermoresponsive polymer inspired by an embryonic induction mechanism, and demonstrates its ability to induce tooth differentiation *in vitro* and *in vivo*. This is effectively a 3D 'shrink wrap'-like polymer sponge that constricts when it is warmed to body temperature and induces compaction of cells contained within it, hence recapitulating the mesenchymal condensation process that has been shown to be a key induction mechanism that triggers formation of various epithelial organs, including tooth in the embryo. The fourth chapter describes the fabrication of a novel microarray screening platform consisting of a unique set of ECM proteins (collagen VI, tenascin, and combination of the two at different coating densities) on an array of soft substrates (~130-1500 Pa) that are physiologically relevant to the embryonic microenvironment.

This technology demonstrated the capacity to analyze combinatorial effects of these ECM proteins and soft substrates on cell density, cell area and odontogenic differentiation in murine mandible embryonic mesenchymal cells. The fifth chapter of this thesis summarizes and discusses the advantages, limitations and future potential of the findings described in the previous two chapters in the context of organ engineering and regeneration. Taken together, the work and results presented in this thesis have led to the development of new insights, approaches and tools for studying organ formation and potentially inducing organ regeneration, which are inspired by key developmental mechanisms used during embryonic organ formation.

Table of Contents

Acknowledgements

In the Name of God, The Most Gracious, The Most Merciful

I thank God, first and foremost, for blessing me with such an amazing and beautiful academic experience at Harvard.

I thank my advisor, Donald Ingber, for his unwavering guidance, support and advice throughout my PhD. Thank you so much for believing in me, encouraging my passion to challenge the impossible in research and academia. It's been an absolute honor and enriching learning experience being your student. I thank my past and current committee members, Dr. Fawwaz Habbal, Professors David Mooney, Ali Khademhosseini, and Neel Joshi. Thank you so much for your invaluable advice and for those pep talks when they were much needed. I thank my collaborators from the Ingber, Aizenberg and Khademhosseini lab: Tada Mammoto, Akiko Mammoto, Amanda Jiang, Professor Joanna Aizenberg, Lauren Zarzar, Keekyoung Kim, and Jalil Zerdani. Thank you for an enriching experience in helping produce such amazing scientific publications. I thank all the staff, faculty and students at the Wyss Institute and Ingber lab, it was truly lovely interacting and even working with some of you. I thank the administrative staff at the Wyss, specifically, Jeannie Nisbet, for going out of her way and working with me side by side to gather some of the world's most brilliant minds in one room for my meetings, and for being genuinely helpful and caring always.

Last but not the least, I thank my family and buzoorgs: Abbu, Ammi, Sahar, Saira, Ibrahim, Maliha, Nada, Bibi Jaan, Mian Bhai, and Qadri Uncle. Thank you for being my inspirations, thank you for your unending love, thank you for everything. Thank you Abbu and Ammi for sharing those inspirational stories of your academic

pursuits from back in the day. Thank you so much for supporting me accomplish this dream of mine.

Finally, I would like to send my sincerest and deepest salutations, peace and God's blessings upon Sayidna Muhammad Peace Be Upon Him, his family and companions, Peace Be Upon Them All. Sallo Alan Nabi Sallalaho Alayhi Wa Salam.

To My Parents, Dr. Nasim A. Hashmi and Aisha Hashmi, My Pyaray Abbu Ammi

Chapter 1:Developmentally Inspired Engineering

Introduction

Organ transplantation remains the major means of replacing lost or severely damaged human organs. However, while the demand for organ transplants continues to grow, the supply can not satisfy this need [1]. To combat this growing problem, Tissue Engineers have strived to design and fabricate synthetic scaffolds that can guide tissue repair, and potentially organ regeneration. Current approaches rely on use of scaffolds composed of synthetic polymers, many of which were originally used for suture materials or non-medical applications, which are coated with extracellular matrix (ECM) adhesive ligands to support cell adhesions. While many different polymer types and configurations have been explored, and there are some tissue engineered constructs approved for clinical use, there have been far more failures than successes in this field.

Most of the tissue engineering scaffolds in the past were designed to mimic the structure of the adult organs which they were designed to replace. My dissertation is based on the hypothesis that we might be able to engineer more effective tissue engineering scaffolds by leveraging design principles that govern how these organs first form in the embryo. With this long-term goal in mind, I have focused on engineering of the tooth organ as a model system. The tooth is ideal for this type of study because of the relative simplicity of its development compared to other organs (e.g., kidney, liver, cartilage, etc.) that similarly rely on a common initiating mechanism that involves a ‘mesenchymal condensation’. This process is when undifferentiated mesenchyme in the early embryo are triggered developmentally to spontaneously cluster together to

form a compact cell mass directly beneath where the first epithelial bud of a new organ (e.g., tooth or liver) will form. The Ingber laboratory in which I carried out my dissertation research recently delineated how mesenchymal condensation is controlled during tooth development, and they discovered that physical compression of the cells during this compaction triggers expression of genes encoding transcription factors that drive tooth development, a process known as 'odontogenesis' [2]. Inspired by this newly defined principle that governs tooth development, I set out to design and fabricate synthetic polymer scaffolds that mimic this mechanical actuation mechanism to artificially engineer tooth formation.

Thus, I begin this dissertation in Chapter 2 with an in depth review of organ regeneration from a developmental perspective, with a specific focus on the mesenchymal condensation process. In Chapter 3, I describe the experimental studies I completed that resulted in the fabrication of a thermoresponsive 'shrink wrap'-like polymer scaffold, which mechanically actuates mesenchymal condensation of embryonic murine mesenchymal cells when warmed to body temperature. I show that this developmentally-inspired polymer scaffold induces these compressed mesenchymal cells to undergo tooth differentiation *in vitro* and form mineralized tissues *in vivo*. In Chapter 4, I describe additional studies I carried out using a modified microarray printing technology to create ECM substrates that vary in their chemistry and mechanics in a controlled manner. These substrates were specifically designed to present a range of mechanical properties (stiffnesses) with greater compliance than any created with this approach in the past to specifically recapitulate the flexibility of embryonic inductive tissues. I show that this technique can be used to screen for

combinations of ECM chemistry and mechanics that produce enhanced induction of tooth differentiation in mesenchymal cells *in vitro*, and hence that might be useful for identification of tissue engineering scaffold design criteria in the future. Finally, in Chapter 5, I summarize the general conclusions that I have gathered from these studies and discuss the future implications of my findings. Please note that Chapter 2-4 are manuscript versions of articles of mine that are respectively in press [3], recently published [4], or soon submitted for publication (manuscript and figures are reprinted with permission from the publishers).

References

[1] Bruno Gridelli, M.D., and Giuseppe Remuzzi M. Strategies for Making More Organs Available for Transplantation. *N Engl J Med* 2000;343:404–10.

[2] Mammoto T, Mammoto A, Torisawa Y, Tat T, Gibbs A, Derda R, Mannix R, de Bruijn M, Yung C, Huh D and Ingber D. Mechanochemical control of mesenchymal condensation and embryonic tooth organ formation. *Dev. Cell* 2011; 21:758-769.

[3] Hashmi B, Mammoto T, and Ingber DE. Developmentally-Inspired Regenerative Organ Engineering: Tooth as a Model. In: Vishwakarma, A, Sharpe P, Shi S, Wang X-P, and Ramalingam M, eds. *Stem Cell Biology and Tissue Engineering in Dental Science.* Elsevier – in press.

[4] Hashmi B, Zarzar L, Mammoto T, Mammoto A, Jiang A, Aizenberg J, and Ingber DE. Developmentally-Inspired Shrink-Wrap Polymers for Induction of Tissue Differentiation. *Adv. Materials* 2014; Feb 18 [Epub ahead of print].

Chapter 2: Developmentally-Inspired Regenerative Organ Engineering: Tooth as a Model

The following chapter is a reproduction of a book chapter I wrote recently for the upcoming book Stem Cell Biology and Tissue Engineering in Dental Science and is currently in press. It has been reproduced with permission.

Hashmi B, Mammoto T, and Ingber DE. Developmentally-Inspired Regenerative Organ Engineering: Tooth as a Model. In: Vishwakarma, A, Sharpe P, Shi S, Wang X-P, and Ramalingam M, eds. *Stem Cell Biology and Tissue Engineering in Dental Science.* Elsevier – in press.

Abstract

Due to rising demands and increasing shortages in organ transplantation, tissue engineers continue to actively investigate methods that could potentially induce organ regeneration in the future. Most engineering approaches attempt to recreate lost organs by using scaffolds that mimic the structure of the adult organ. However, tooth organ formation in the embryo results from complex interactions between adjacent epithelial and mesenchymal cells that produce whole teeth through sequential induction steps and progressive remodeling of increasing complex three-dimensional tissue structures. Using the tooth as a model and blueprint for regenerative organ engineering, this chapter reviews the key role that epithelial-mesenchymal interactions, associated mesenchymal condensation and mechanical forces play in odontogenesis in the embryo. We also discuss dental engineering strategies currently under development that are inspired by this induction mechanism, which employ extracellular matrix proteins and mechanically active polymer scaffolds to induce tooth formation *in vitro* and *in vivo*.

Keywords: *tooth, odontogenesis, regeneration, tissue engineering, organ engineering, polymer scaffold, mesenchymal condensation, epithelial-mesenchymal interactions*

Introduction

Organ transplantation continues to pose a major problem worldwide[1]. More than 100,000 patients require organ transplantation every year in the U.S. alone; however, due to a supply-demand imbalance, close to 20 humans die every day while waiting for organ transplants. For this reason, the ultimate goal in the fields of Tissue Engineering and Regenerative Medicine is regenerate whole organs in order to restore lost physiological and structural functions. Existing regenerative engineering approaches commonly rely on the use of tissue-specific cells from adult tissues or multi-potential stem cells, either alone or in combination with three-dimensional (3D) adhesive scaffolds that mimic the microstructure of the organ that is to be replaced or repaired[2,3]. Significant progress has been made in producing biomaterials to repair simple tissues (e.g., skin, cartilage or bone)[4,5]; however, these approaches still remain limited in achieving complete organ regeneration. One of the major challenges in this field is that existing tissue engineering approaches are focused on rebuilding adult tissues rather than recapitulating the way in which organs initially form (i.e., in the embryo). Therefore, it is important to identify the key factors and control processes that govern embryonic organ, and to leverage them to develop more effective design criteria for organ engineering strategies.

Understanding Generation for Regeneration Strategies: A Tooth Model

One of the simplest model systems for studying mammalian organ formation is the tooth, which is an organ responsible for mastication. The tooth, like other organs, is compromised of epithelium, connective tissue, nerves, blood vessels, ligaments as well as specialized extracellular matrix (ECM), in this case, the hard, bone-like covering

tissues of the tooth dentin and enamel. However, the simplicity of this organ makes it an excellent model for studying and understanding organ regeneration. As in the development of many other epithelial organs, the tooth forces through reciprocal interactions between the epithelium and mesenchyme that lead to condensation of the mesenchyme and subsequent budding and differentiation of the overlying epithelium to form the complex structure of the organ [6–9]. However, the simplicity of the budding process makes tooth especially amenable to experimental analysis. If we could uncover the principles necessary to regenerate a fully functionally tooth, it would likely also have important implications for engineering other epithelial organs that utilize similar developmental processes, such as bone, cartilage, kidney, pancreas, and heart.

Apart from understanding and attempting to engineer organ regeneration in the lab, tooth regeneration is of critical importance for dental medicine. Teeth ailments can range from simple dental caries to more serious genetic defects, such as agenesis (the failure to form teeth), the effects of which can be physically and mentally debilitating[10].In fact, missing teeth are one of the most common developmental problems in children who are not eligible for dental implants. This is because their jawbones are immature and actively growing; as a result, 20% of children aged 9 to 11 have one or more missing permanent teeth in the United States[11]. Thus, development of a tissue engineering approach that could effectively regenerate teeth could have a significant positive impact on clinical dentistry.

Many of the genes and chemical cues that mediate tissue and organ development have been identified; however, these signals alone are not sufficient to explain how tissues and organs are constructed so that they exhibit their unique

material properties and 3D forms. It is becoming clear that organ development is a mechanochemical process in which masses of cells are shaped into functional organs through reciprocal physical and chemical interactions between epithelial and mesenchymal tissues, and this is particularly evident in the key role that mesenchymal cell compaction plays during tooth organ induction[6,7,12]. Recently a new class of multifunctional biomaterials was developed with unique mechanical actuation capabilities that can recapitulate key developmental biological events that occur during the mesenchymal condensation response, which are required for induction of tooth tissue and organ formation in the embryo[8]. This biologically-inspired engineering approach recapitulates key developmental processes synthetically. Thus, in this chapter, we will discuss the how an increased understanding of developmental biology is being leveraged to develop entirely new biomaterials and engineering approaches for regenerative dental medicine.

Epithelial-Mesenchymal Interactions During Odontogenesis

Embryonic organ formation is a mechanochemical process in which masses of cells are shaped into functional organs through reciprocal interactions controlled by mechanical as well as chemical cues[6,7]. This is evident in the inductive tissue interactions between apposed epithelial and mesenchymal tissue layers that are responsible for directing formation of many organs during vertebrate development[9]. For example, during the formation of many epithelial organs (e.g., tooth, lung, pancreas, kidney, heart valve, breast, salivary gland, bone, cartilage and hair follicle), instructive signals provided by the epithelium are transferred to the mesenchyme through key morphogenetic movements that result in a dense packing of mesenchymal cells, or

what is known as ‘mesenchymal condensation’. Classic and recent embryological studies have shown that this process is crucial for the formation of many organs[9,13–16].

Odontogenesis, or tooth organ formation, provides one of the simplest examples of how this fundamental development control mechanism works. Physical compaction of the early dental mesenchymal cells shifts the inductive capacity for odontogenesis from the dental epithelium to the mesenchyme *in vitro*[12]. Specifically, during embryonic days 10 to 12 (E10-12) in the mouse, the initial “potential” for tooth formation resides within the dental epithelium, as heterotopic recombination of this epithelium with undifferentiated embryonic mesenchyme or with adult bone marrow-derived mesenchymal stem cells (aMSCs), results in formation of a differentiated tooth containing roots, dentin and enamel when the tissue recombinant is implanted into living mice[17,18]. However, by E13, the dental epithelium’s inductive power is transferred to the previously undifferentiated dental mesenchyme, which is then capable of stimulating adjacent undifferentiated epithelium to form a tooth[19]. Moreover, this inductive mesenchyme also appears to contain all of the information necessary to induce formation a whole tooth even when combined with epithelium isolated from non-dental buccal regions from adult mouse and implanted *in* vivo[12].

As epithelial-mesenchymal interactions are crucial for tooth organ formation, it is critical to understand how this process works in the embryo in order to apply these principles to organ engineering. Studies carried out fifty years analyzing tooth development first identified the odontogenic developmental capabilities of the epithelium and mesenchyme, and these investigators even attempted to regenerate a tooth in

vitro[20–25]. For example, when the oral epithelium and mesenchyme from day 20 gestation white rabbits were reconstituted in the highly vascularized chick chorio-allantoic membrane, formation of dentin-enamel junctions resulted[25]. However, it wasn't until nearly two decades later that the inductive capability of the oral embryonic epithelium was first identified by demonstrating the ability of mandibular epithelium isolated from mouse embryos to stimulate an odontogenic response in non-dental mesenchyme[17].

Interestingly, the dental epithelium starts losing this inductive ability after E12, and there is a concomitant increase in the ability of the dental mesenchyme to induce whole tooth formation when recombined with non-dental epithelium and implanted *in vivo*[19]. These findings suggest that the early (<E13) DE programs undifferentiated non-dental mesenchymal cells to pursue the odontogenic lineage, and that the inductive ability, which resides primarily in early epithelium is subsequently transferred to the underlying mesenchyme at ~E13, which then drives subsequent stages of tooth development. For example, the embryonic epithelium has been shown to reprogram non-dental mesenchymal stem cells to express odontogenic genes[18].Moreover, once the mesenchymal cells are programmed to become inductive (i.e., mimic the shift of inductive capacity normally observed on E13 in the embryo), there are able to induce full tooth differentiation when combined with embryonic dental epithelium an implanted under the kidney capsule in an adult mouse. The key genes that are expressed in the inductive mesenchyme at E13 have been identified as Pax9, Msx1, Bmp4, among others[9,12,19,26–28].This development processes inspired additional studies in which the oral epithelium and mesenchyme were physically separated, then recombined in

vitro, implanted under the kidney capsule to form a tooth rudiment, and finally this was transplanted to the oral cavity resulting formation of a functional tooth in a mouse [29] (Figure 2.1).

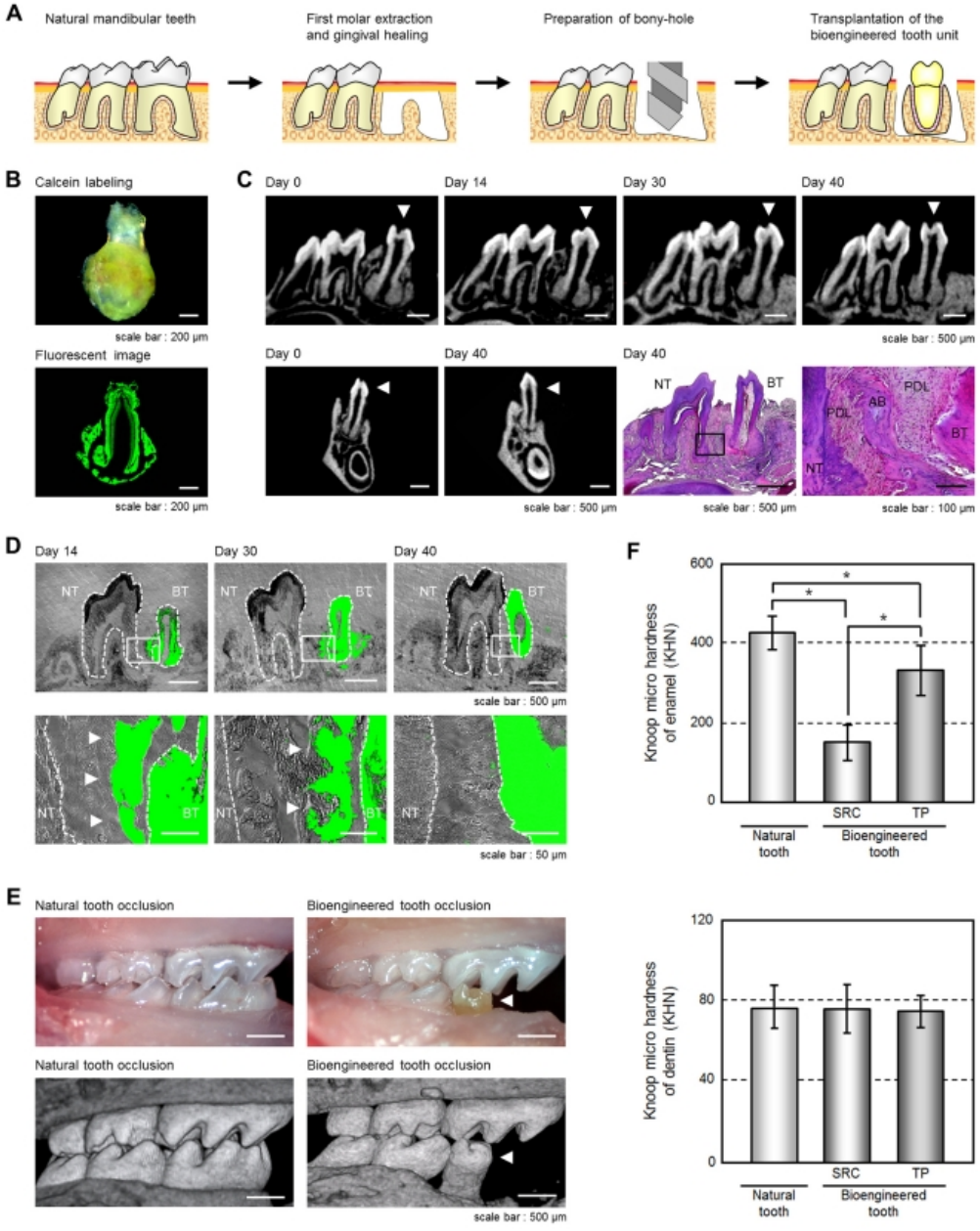

Figure 2.1 Engraftment and occlusion of a bioengineered tooth unit in a tooth loss model. A) Schematic representation of the protocol used to transplant a bioengineered tooth unit in a murine tooth loss model. B) Photograph (upper) and

Figure 2.1 (Continued)…sectional image (lower) of a calcein-labeled bioengineered tooth unit at 60 days post transplantation in the subrenal capsule (bar, 200 mm). C) Micro-computerized tomography (micro-CT) images of a bioengineered tooth unit (arrowhead) in cross section (upper) and frontal section (first and second figures from the lower left) during the processes of bone remodeling and connection between the recipient jaw bone and alveolar bone of the tooth unit. Histological analysis of the engrafted bioengineered tooth unit at 40 days post transplantation was also performed (bar, 500 mm and 100 mm in the third and fourth figure from the lower left; NT, natural tooth; BT, bioengineered tooth; AB, alveolar bone; PDL, periodontal ligament). D) Sectional images of a calcein-labeled bioengineered tooth unit at 14, 30 and 40 days post-transplantation. The calcein-labeled bone of the bioengineered tooth units (arrowhead) was found to gradually decrease from the outside and finally disappear at 40 days post-transplantation (bar, 500 mm (upper), 50 mm (lower); NT, natural tooth; BT, bioengineered tooth. E) Oral photographs (upper) and micro-CT (lower) images showing occlusion of natural (left) and bioengineered teeth (right) (bar, 500 mm). F) Knoop microhardness values of the enamel (upper) and dentin (lower) of a bioengineered tooth measured at 60 days post-transplantation in a subrenal capsule (SRC), and at 40 days post-transplantation in jawbone (TP) were compared with those of natural teeth in 11-week-old mice to assess the hardness of the bioengineered tooth. [Error bars indicate standard deviation; *P, 0.01; reproduced with permission from ref. 29].

Finally, most recently, these findings were confirmed and, in addition, the early epithelium was shown to be able to induce adult bone marrow-derived stem cells (BMSCs) to undergo odontogenesis [12]. Importantly, this study also revealed that mechanical forces play a central role in this transfer of inductive capacity that accompanies mesenchymal condensation. Specifically, analysis of embryonic tooth formation in the mouse revealed that the early dental epithelium induces mesenchymal condensation by secreting two soluble morphogens, the motility-promoting factor Fgf8 and motility inhibitor Sema3f. A gradual gradient of Fgf8 attracts distant mesenchymal cells to move towards the epithelium, while a steep gradient of Sema3f prevents their subsequent movement and results in formation of a tightly packed mesenchymal cell mass. These studies also revealed that this physical cell compaction induces expression of Pax9 that drives odontogenesis in a RhoA-dependent manner. Most importantly mechanical compression of mesenchymal cells alone was shown to be sufficient to trigger odontogenesis in vitro and induce tooth organ formation in vivo [12] (Figure 2.2).

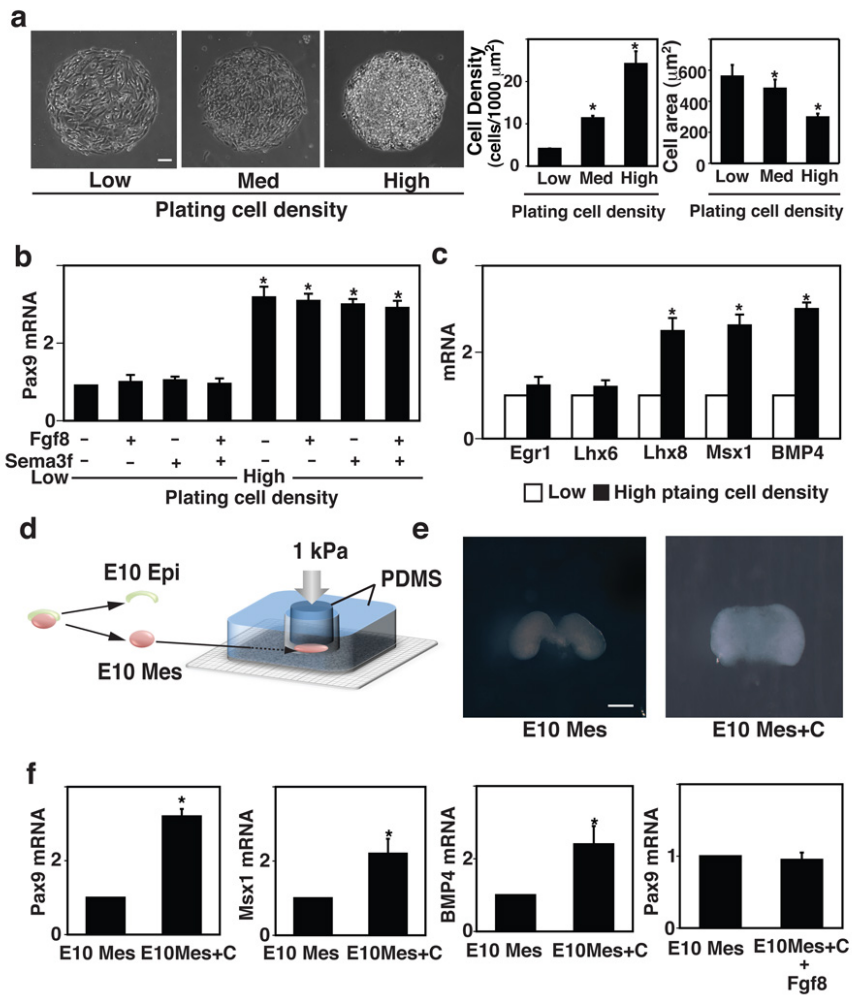

Figure 2.2 Mechanical control of odontogenic transcription factors during tooth development. a) Phase contrast micrographs (left) showing mesenchymal cells cultured for 16 h on microfabricated circular fibronectin (FN) islands (500 μm diameter) *in vitro* at low, medium or high plating cell density (0.2, 1.2 or 2.4 × 10^5 cells/cm^2, respectively), and graphs at right showing corresponding cell densities and projected cell areas (bars, 50 μm). b) Graph showing Pax9 induction in mesenchymal cells cultured for 16 h on the circular FN islands (500 μm diameter) at low or high plating density with or without Fgf8 (150 ng/ml) and/or Sema3f (150 ng/ml). c) Graph showing induction of additional odontogenic factors (Egr1, Lhx6, Lhx8,

Figure 2.2 (Continued)…Msx1 and BMP4) in mesenchymal cells cultured under the same conditions as in b.d) Freshly isolated E10 mesenchyme from first pharyngeal arch was physically compressed (1 kPa) for 16 h using a mechanical compressor composed of two pieces of PDMS polymer that are overlaid with a metal weight. e)Macroscopic images of mesenchyme that was cultured *ex vivo* for 16 h in the absence (E10 Mes) or presence of compression (E10 Mes+C) (bar, 500 μm). f) Graph showing expression of Pax9, Msx1 and BMP4 mRNAs in control (E10 Mes) versus compressed mesenchyme (E10 Mes+C) and expression of Pax9 in control mesenchyme versus mesenchyme treated with soluble Fgf8 (150 ng/ml) for 16 h. [In all figures, *, $p < 0.01$; figure reproduced with permission from ref. 12].

Thus, it might be possible to develop tissue engineering approaches that harness this mechanical actuation to induce tooth organ formation, as will be described below.

ECM and Mechanical Forces as Regulators of Organogenesis

ECM scaffolds that support cell adhesion at the interface between interacting epithelium and mesenchyme undergo dynamic remodeling during organogenesis [30–34]. In addition to serving as an attachment scaffold, the ECM also modulates physical force distributions in cells and tissues based on its ability to resist and balance cell traction forces, and thereby control cell and cytoskeletal shape[35–37]. Importantly, changes in cell shape, in turn, modulate the sensitivity of cells to the chemical factors and thereby, govern cell fate switching[38,39]. In this manner, physical forces transmitted over ECM and to cells control development processes including growth, migration, differentiation, contractility, apoptosis, lineage specification, and cellular self

assembly [7,38,40–50]. ECM mechanics and the physical microenvironment are also critical determinants of stem cell fate. For example, ECM mechanics has been shown to direct mesenchymal stem cells (MSCs) along different stem lineages (e.g., bone, muscle, fat, nerve) based on the stiffness of the ECM substrate[44]. These effects are mediated by changes in activity of the small GTPase RhoA, inside the cell, and in MSCs for example, inhibition and activation of RhoA stimulate adipogenic and osteogenic differentiation, respectively [49].

ECM also orients many growth factors, and some morphogens that play crucial roles in shifting the inductive capability from the dental epithelium to the mesenchyme in the embryo[51], such as Wnts and BMPs, also have been shown to associate with the ECM[52,53]. For example, using gene microarrays and proteomics combined with an informatics approach, multiple morphogens have been identified that exhibit increased expression during the critical phase of development when the inductive ability shifts from the dental epithelium to its mesenchyme. Wnts (Wnt4, Wnt6, Wnt7b, Wnt10a), Fgfs (Fgf4, Fgf8) and BMP4 all appear to play key roles in shifting of the inductive ability from the epithelium to the mesenchyme in the tooth germ at E13-14, in addition to the transcription factors Pax9 and Msx1 that were previously known to mediate this process[12,51,54].Furthermore, these studies revealed that mRNA levels for a number of ECM components (e.g., collagen I, III, IV, VI, emilin, fibulin, laminin, tenascin C and versican) also increase in condensed dental mesenchyme at E13-14 compared to undifferentiated mesenchyme at E10[12].

Further analysis of the condensing mesenchyme in the form tooth revealed that it accumulates an ECM rich in type VI collagen during this induction process, and

importantly, inhibition of collagen accumulation inhibits tooth differentiation in this model[12]. Thus, ECM appears to play a key role in tooth development during this early induction phase by sustaining differentiation processes that are triggered physically by mesenchymal cell compaction. Thus, as the physical and chemical properties of ECM are extremely important for tooth development, this knowledge must be leveraged for organ engineering as well. Interestingly, whole adult organs (e.g., lung, heart, liver) have been successfully engrafted *in vivo* by first detergent-extracting the organs to isolate their natural ECM scaffolds and then repopulating them with progenitor cells[55–61]; however, this extraction method has not yet been carried out with tooth.

Engineering Approaches for Tooth Organ Regeneration

To recapitulate the endogenous regenerative capabilities of dental tissue, past tissue engineering approaches have largely focused on the importance of chemical factors and biomaterials for inducing tooth regeneration[62–64]. Synthetic scaffolds that have been explored for this purpose generally employ natural ECM components or synthetic polymers that exhibit high biocompatibility, low immunogenicity, high adhesive capacity, and controllable degradability *in vivo*. These scaffolds have been fabricated from collagen, hyaluronic acid, chitosan, alginate, fibrin, and silk among others[63,65–71]; however, they all are limited in their functionality and mechanical strength. Other synthetic biocompatible polymers that are stronger more robust, and currently used for dental applications, such as polylactide-co-glycolide (PLGA), hydroxyapatite, polyglycolic acid (PGA) also have been explored for this purpose[62,72–74]. But most of these synthetic polymers have many limitations as well, including their inability to

support cell adhesion without chemical modification, undesired induction of immunogenic responses, and release of toxic by-products during degradation.

One potential way to circumvent these limitations would be to develop scaffolds inspired by development that recapitulate key features of the mesenchymal condensation process that drives tooth formation in the embryo[8]. Past studies that attempted to induce mesenchymal cell compaction by exposing the cells to the morphogens that drive these processes in the embryo did not prove successful[12]. Recently, a synthetic 'mechanically-actuatable' scaffold was developed that successfully stimulated compaction of embryonic dental mesenchymal cells, induced expression of key odontogenic genes, and stimulated tooth tissue formation *in vitro* and *in vivo*[8]. In this study, undifferentiated embryonic mesenchymal cells from the mouse mandible were injectedat room temperature within the pores of a thermoresponsivepoly(*N*-isopropylacrylamide) (PNIPAAm) hydrogel composed of 10% *N*-isopropylacrylamide (NIPAAm) monomer and 1% *N,N'*–methylenebisacrylamide (BIS), which was chemically modified with RGD-containing adhesive peptide. This gel autonomously contracts in 3D when warmed to body temperature (37^{o}C), which causes the mesenchymal cells to round and take on the morphology of a condensed mesenchyme in the embryo. This mechanical compaction response was shown to be sufficient to induce expression of the key odontogenic transcription factor Pax9 *in vitro* and to stimulate formation of mineralized tooth tissue *in vivo*[8] (Figure 2.3).

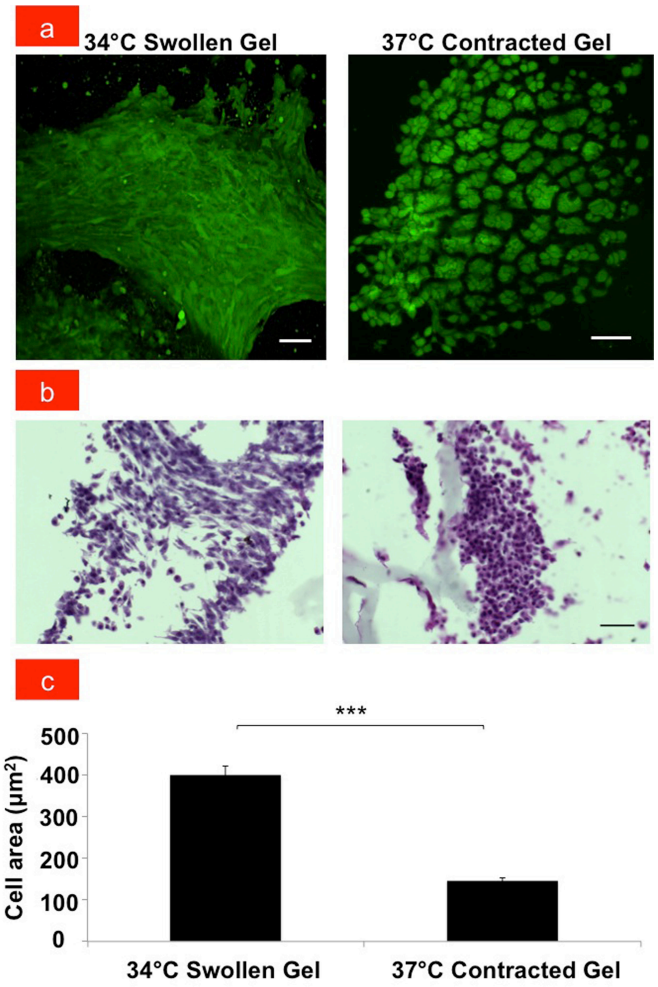

Figure 2.3 Induction of mesenchymal condensation and tooth differentiation using a developmentally-inspired, shrink-wrap, polymer gel. a) Fluorescent micrographs of E10 dental mesenchymal cells grown overnight in swollen GRGDS-PNIPAAm hydrogel at 34°C versus in contracted GRGDS-PNIPAAm hydrogel at 37°C (bar, 50 μm). b) Light micrographs showing hematoxylin and eosin (H&E) staining of the mesenchymal cells that appear spread in the swollen GRGDS-PNIPAAm hydrogel, whereas they are compact and rounded in the contracted GRGDS-PNIPAAm hydrogel at 37°C (bar, 50 μm). c) Graph showing the quantification of the corresponding projected cell areas; ***p<0.001. [Reproduced with permission from ref. 8.]

Exploration of the full potential of this new developmentally-inspired approach to tooth engineering will require that similar studies be carried out in combination with epithelium and both tissue (epithelium and induced mesenchyme) have been show to be required for tooth formation in tissue recombination experiments[12,18,29]. Nevertheless, these findings provide the proof-of-principle for developing organ engineering approaches that recapitulate normal developmental process that are initially used to drive organ formation in the embryo. They also demonstrate the importance of focusing on mechanical design criteria, as well as chemical features, when devising new tissue engineering biomaterials.

Conclusion

While significant advances have been in the engineering of some tissues (e.g. skin, cartilage), there is still a major void between current capabilities and the field's ultimate goal of regenerating whole human organs de novo. This is likely due in large part to our inability to effectively recapitulate the key features of the local tissue microenvironment that are crucial for organ formation. Most of the past focus in this field has been on creation of synthetic polymer scaffolds that mimic the architecture of adult tissue, addition of important soluble morphogens, and delivery of regenerative stem cells. While there have been some small successes in terms of stimulating tissue repair, there is still a great need for alternative approaches that are more effective at induce true organ regeneration.

Developmentally-inspired approaches to tooth organ engineering represent a potentially exciting new path to pursue in this area. The discovery that the physical compaction of undifferentiated mesenchymal cells is the key signal that mediates the

shift of odontogenic inductive capability from the dental epithelium to the mesenchyme at E12-13 provides a fundamental new insight into how organs develop[12]. The level of tooth differentiation produced by these shrink wrap-like polymers also might be enhanced in the future by incorporating ECM components and growth factors that are important for sustaining tooth development in the embryo, and by combining epithelium with the condensed mesenchyme. If this can be demonstrated with adult MSCs or dental pulp stem cells, then this could represent a viable new approach to tissue engineering in vivo.

Importantly, the development of mechanically-actuable polymers that induce tooth tissue formation by mimicking the mesenchymal condensation response represents a major departure from most biomaterial engineering strategies used for regenerative medicine, which primarily focus on design and optimization of scaffold chemistry and structure[75,76]. In the future, it also might be possible to manipulate the size and shape of teeth that are formed by altering the shape of the scaffolds given that the size and shape of the condensed cell mass have been shown to dictate the final 3D form of the organ[15,77]. Moreover, as mesenchymal condensation is required for induction of many types of epithelial organs, this bioinspired mechanical actuation system could be broadly useful for control of stem cell function, tissue engineering and regenerative medicine.

References

1. Bruno Gridelli, M.D., and Giuseppe Remuzzi M. Strategies for Making More Organs Available for Transplantation. N Engl J Med. 2000;343:404–10.

2. Ingber DE, Mow VC, Butler D, Niklason L, Huard J, Mao J, Yannas I, Kaplan D, Vunjak-Novakovic G. Tissue engineering and developmental biology: going biomimetic. Tissue Eng. 2006;12(12):3265–83.

3. Howard D, Buttery LD, Shakesheff KM, Roberts SJ. Tissue engineering: strategies, stem cells and scaffolds. J Anat. 2008;213(1):66–72.

4. Navarro M, Michiardi A, Castaño O, Planell J a. Biomaterials in orthopaedics. J R Soc Interface. 2008;5(27):1137–58.

5. Chen F-M, Zhang J, Zhang M, An Y, Chen F, Wu Z-F. A review on endogenous regenerative technology in periodontal regenerative medicine. Biomaterials.2010;31(31):7892–927.

6. Mammoto T, Ingber DE. Mechanical control of tissue and organ development. Development.2010;137(9):1407–20.

7. Mammoto T, Mammoto A, Ingber DE. Mechanobiology and developmental control. Annu Rev Cell Dev Biol. 2013;29:27–61.

8. Hashmi B, Zarzar LD, Mammoto T, Mammoto A, Jiang A, Aizenberg J, Ingber DE. Developmentally-Inspired Shrink-Wrap Polymers for Mechanical Induction of Tissue Differentiation. Adv Mater. 2014[epub ahead of print]

9. Thesleff I. Epithelial-mesenchymal signalling regulating tooth morphogenesis. J Cell Sci. 2003;116(9):1647–8.

10. Nakahara T, Ide Y. Tooth regeneration: implications for the use of bioengineered organs in first-wave organ replacement. Hum Cell. 2007;20(3):63–70.

11. White JA, Beltran ED, Malvitz DM, Perlman SP. Oral health status of special athletes in the San Francisco Bay Area. J Calif Dent Assoc. 1998;26:347–54.

12. Mammoto T, Mammoto A, Torisawa Y, Tat T, Gibbs A, Derda R, Mannix R, de Bruijn M, Yung CW, Huh D, Ingber DE. Mechanochemical control of mesenchymal condensation and embryonic tooth organ formation. Dev Cell.2011;21(4):758–69.

13. Smith MM, Hall BK. Development and evolutionary origins of vertebrate skeletogenic and odontogenic tissues. Biol Rev Camb Philos Soc. 1990;65:277–373.

14. Hall BK, Miyake T. Divide, accumulate, differentiate: cell condensation in skeletal development revisited. Int J Dev Biol.1995;39(6):881–93.

15. Hall BK, Miyake T. The membranous skeleton : the role of cell condensations in vertebrate skeletogenesis. Anat Embryol (Berl). 1992;186(2):107–24.

16. Hall BK, Miyake T. All for one and one for all: condensations and the initiation of skeletal development. Bioessays. 2000;22(2):138–47.

17. Mina M, Kollar E. The induction of odontogenesis in non-dental mesenchyme combined with early murine mandibular arch epithelium. Arch Oral Biol. 1987;32:123–7.

18. Ohazama a., Modino S a. C, Miletich I, Sharpe PT. Stem-cell-based Tissue Engineering of Murine Teeth. J Dent Res. 2004;83(7):518–22.

19. Maas R, Bei M. The Genetic Control of Early Tooth Development. Crit Rev Oral Biol Med [Internet]. 1997;8(1):4–39.

20. Grobstein C. Mechanisms of organogenetic tissue interaction. Natn Cancer Inst Monogr. 1967;26:279–99.

21. Koch WE. In vitro differentiation of tooth rudiments of embryonic mice. I. Transfilter interaction of embryonic incisor tissues. J Exp Zool. 1967;165(2):155–69.

22. Slavkin HC, Bringas P, Cameron J, LeBaron R, Bavetta L a. Epithelial and mesenchymal cell interactions with extracellular matrix material in vitro. J Embryol Exp Morphol. 1969;22(3):395–405.

23. Slavkin HC, Bavetta LA. Odontogenesis in vivo and in xenografts on chick chorio-allantois. I. Collagen and hexosamine biosynthesis. Arch Oral Biol. 1968;13:145–54.

24. Kollar EJ, Baird GR. The influence of the dental papilla on the development of tooth shape in embryonic mouse tooth germs. J Embryol Exp Morphol. 1969;21(1):131–48.

25. Slavkin H, Beierle J, Bavetta L. Odontogenesis: cell-cell interactions in vitro. Nature. 1968;217:269–70.

26. Ohazama A, Modino SAC, Miletich I, Sharpe PT. Stem-cell-based tissue engineering of murine teeth. J Dent Res. 2004;83:518–22.

27. Thesleff I. Developmental biology and building a tooth. Quintessence Int. 1985;34(8):613–20.

28. Jernvall J, Thesleff I. Tooth shape formation and tooth renewal: evolving with the same signals. Development. 2012;139(19):3487–97.

29. Oshima M, Mizuno M, Imamura A, Ogawa M, Yasukawa M, Yamazaki H, Morita R, Ikeda E, Nakao K, Takano-Yamamoto T, Kasugai S, Saito M, Tsuji T. Functional tooth regeneration using a bioengineered tooth unit as a mature organ replacement regenerative therapy. PLoS One. 2011;6(7):e21531.

30. Kramer KL, Yost HJ. Ectodermal syndecan-2 mediates left-right axis formation in migrating mesoderm as a cell-nonautonomous Vg1 cofactor. Dev Cell. 2002;2(1):115–24.

31. Rifes P, Thorsteinsdóttir S. Extracellular matrix assembly and 3D organization during paraxial mesoderm development in the chick embryo. Dev Biol. 2012;368(2):370–81.

32. Rozario T, DeSimone DW. The extracellular matrix in development and morphogenesis: a dynamic view. Dev Biol. 2010;341(1):126–40.

33. Skoglund P, Keller R. Xenopus fibrillin regulates directed convergence and extension. Dev Biol. 2007;301(2):404–16.

34. Yin C, Kikuchi K, Hochgreb T, Poss KD, Stainier DYR. Hand2 regulates extracellular matrix remodeling essential for gut-looping morphogenesis in zebrafish. Dev Cell.2010;18(6):973–84.

35. Ingber DE, Jamieson JD. Cells as tensegrity structures: architectural regulation of histodifferentiation by physical forces tranduced over basement membrane. In: Andersson L, Gahmberg C, Ekblom P, editors. Gene Expression During Normal and Malignant Differentiation. Waltham, MA: Academic; 1985.

36. Beloussov L V, Louchinskaia NN, Stein a a. Tension-dependent collective cell movements in the early gastrula ectoderm of Xenopus laevis embryos. Dev Genes Evol. 2000 Feb;210(2):92–104.

37. Huang S, Ingber DE. The structural and mechanical complexity of cell-growth control. Nat Cell Biol. 1999;1(5):E131–8.

38. Chen CS, Mrksich M, Huang S, Whitesides GM, Ingber DE. Geometric control of cell life and death. Science. 1997;276(5317):1425–8.

39. Dike LE, Chen CS, Mrksich M, Tien J, Whitesides GM, Ingber DE. Geometric control of switching between growth, apoptosis, and differentiation during angiogenesis using micropatterned substrates. In Vitro Cell Dev Biol Anim. 1999;35(8):441–8.

40. Ingber DE, Folkman J. How Does Extracellular Matrix Control Capillary Morphogenesis ? Minireview. Cell. 1989;58:803–5.

41. Alcaraz J, Xu R, Mori H, Nelson CM, Mroue R, Spencer V a, Brownfield D, Radisky DC, Bustamante C, Bissell MJ. Laminin and biomimetic extracellular elasticity enhance functional differentiation in mammary epithelia. EMBO J. 2008;27(21):2829–38.

42. Polte TR, Eichler GS, Wang N, Ingber DE. Extracellular matrix controls myosin light chain phosphorylation and cell contractility through modulation of cell shape and cytoskeletal prestress. Am J Physiol Cell Physiol. 2004;286(3):C518–28.

43. Mammoto T, Ingber DE. Mechanical control of tissue and organ development. Development. 2010;137(9):1407–20.

44. Engler AJ, Sen S, Sweeney HL, Discher DE. Matrix elasticity directs stem cell lineage specification. Cell [Internet]. 2006;126(4):677–89.

45. Guo C, Ouyang M, Yu J, Maslov J, Price A, Shen C. Long-range mechanical force enables self-assembly of epithelial tubular patterns. Proc Natl Acad Sci U S A. 2012;109:5576–82.

46. Hadjipanayi E, Mudera V, Brown R a. Guiding cell migration in 3D: a collagen matrix with graded directional stiffness. Cell Motil Cytoskeleton. 2009;66(3):121–8.

47. Kadler K. Matrix loading: assembly of extracellular matrix collagen fibrils during embryogenesis. Birth Defects Res C Embryo Today. 2004;72(1):1–11.

48. Lo CM, Wang HB, Dembo M, Wang YL. Cell movement is guided by the rigidity of the substrate. Biophys J. Elsevier; 2000;79(1):144–52.

49. McBeath R, Pirone DM, Nelson CM, Bhadriraju K, Chen CS. Cell shape, cytoskeletal tension, and RhoA regulate stem cell lineage commitment. Dev Cell. 2004;6(4):483–95.

50. Parker KK, Brock AL, Brangwynne C, Mannix RJ, Wang N, Ostuni E, Geisse N a, Adams JC, Whitesides GM, Ingber DE. Directional control of lamellipodia extension by constraining cell shape and orienting cell tractional forces. FASEB J. 2002;16(10):1195–204.

51. O'Connell DJ, Ho JWK, Mammoto T, Turbe-Doan A, O'Connell JT, Haseley PS, Koo S, Kamiya N, Ingber DE, Park PJ, Maas RL. A Wnt-bmp feedback circuit controls intertissue signaling dynamics in tooth organogenesis. Sci Signal.2012;5(206):ra4.

52. Reichsman F, Smith L, Cumberledge S. Glycosaminoglycans Can Modulate ExtraceUular Localization of the. J Cell Biol. 1996;135(3):819–27.

53. Hynes RO. The extracellular matrix: not just pretty fibrils. Science. 2009;326(5957):1216–9.

54. Wang X-P, O'Connell DJ, Lund JJ, Saadi I, Kuraguchi M, Turbe-Doan A, Cavallesco R, Kim H, Park PJ, Harada H, Kucherlapati R, Maas RL. Apc inhibition of Wnt signaling regulates supernumerary tooth formation during embryogenesis and throughout adulthood. Development.2009;136(11):1939–49.

55. Ott HC, Clippinger B, Conrad C, Schuetz C, Pomerantseva I, Ikonomou L, Kotton D, Vacanti JP. Regeneration and orthotopic transplantation of a bioartificial lung. Nat Med.2010;16(8):927–33.

56. Ott HC, Matthiesen TS, Goh S-K, Black LD, Kren SM, Netoff TI, Taylor D a. Perfusion-decellularized matrix: using nature's platform to engineer a bioartificial heart. Nat Med. 2008;14(2):213–21.

57. Petersen TH, Calle E a, Zhao L, Lee EJ, Gui L, Raredon MB, Gavrilov K, Yi T, Zhuang ZW, Breuer C, Herzog E, Niklason LE. Tissue-engineered lungs for in vivo implantation. Science. 2010;329(5991):538–41.

58. Uygun BE, Soto-Gutierrez A, Yagi H, Izamis M-L, Guzzardi M a, Shulman C, Milwid J, Kobayashi N, Tilles A, Berthiaume F, Hertl M, Nahmias Y, Yarmush ML, Uygun K. Organ reengineering through development of a transplantable recellularized liver graft using decellularized liver matrix. Nat Med. 2010;16(7):814–20.

59. Baptista PM, Siddiqui MM, Lozier G, Rodriguez SR, Atala A, Soker S. The use of whole organ decellularization for the generation of a vascularized liver organoid. Hepatology. 2011;53(2):604–17.

60. Nakayama KH, Batchelder CA, Ph D, Lee CI, Ph D, Tarantal AF, Ph D. Decellularized Rhesus Monkey Kidney as a Three-Dimensional Scaffold for Renal Tissue Engineering. Tissue Eng Part A. 2010;16(7):2207–16.

61. Baptista PM, Orlando G, Mirmalek-Sani S-H, Siddiqui M, Atala A, Soker S. Whole organ decellularization - a tool for bioscaffold fabrication and organ bioengineering. Conf Proc IEEE Eng Med Biol Soc. 2009 Jan;2207–16.

62. Bohl K, Shon J, Rutherford B, Mooney DJ. Role of synthetic extracellular matrix in development of engineered dental pulp. J Biomater Sci Polym Ed. 1998;9:749–64.

63. Boynueğri D, Ozcan G, Senel S, Uç D, Uraz A, Oğüş E, Cakilci B, Karaduman B. Clinical and radiographic evaluations of chitosan gel in periodontal intraosseous defects: a pilot study. J Biomed Mater Res B Appl Biomater. 2009;90(1):461–6.

64. Tonomura A, Mizuno D, Hisada A, Kuno N, Ando Y, Sumita Y, Honda MJ, Satomura K, Sakurai H, Ueda M, Kagami H. Differential effect of scaffold shape on dentin regeneration. Ann Biomed Eng. 2010;38(4):1664–71.

65. Nakashima M. Induction of dentine in amputated pulp of dogs by recombinant morphogenetic proteins-2 and -4 with collagen matrix. 1994;39(12):1085–9.

66. Sumita Y, Honda MJ, Ohara T, Tsuchiya S, Sagara H, Kagami H, Ueda M. Performance of collagen sponge as a 3-D scaffold for tooth-tissue engineering. J Biomater Sci Polym Ed. 2006;27(17):3238–48.

67. Lee KY, Mooney DJ. Hydrogels for Tissue Engineering. Chem Rev. 2001;101(7):1869–80.

68. Alsberg E, Anderson KW, Albeiruti a., Franceschi RT, Mooney DJ. Cell-interactive Alginate Hydrogels for Bone Tissue Engineering. J Dent Res. 2001;80(11):2025–9.

69. Yang KC, Wang CH, Chang HH, Chan WP, Chi CH, Kuo TF. Fibrin glue mixed with platelet-rich fibrin as a scaffold seeded with dental bud cells for tooth regeneration. J Tissue Eng Regen Med. 2012;6:777–85.

70. Xu W-P, Zhang W, Asrican R, Kim H-J, Kaplan DL, Yelick PC. Accurately shaped tooth bud cell-derived mineralized tissue formation on silk scaffolds. Tissue Eng Part A. 2008;14(4):549–57.

71. Inuyama Y, Kitamura C, Nishihara T, Morotomi T, Nagayoshi M, Tabata Y, Matsuo K, Chen K-K, Terashita M. Effects of hyaluronic acid sponge as a scaffold on odontoblastic cell line and amputated dental pulp. J Biomed Mater Res B Appl Biomater. 2010;92(1):120–8.

72. Duailibi MT, Duailibi SE, Young CS, Bartlett JD, Vacanti JP, Yelick PC. Bioengineered Teeth from Cultured Rat Tooth Bud Cells. J Dent Res. 2004;83(7):523–8.

73. Young CS, Abukawa H, Asrican R, Ravens M, Troulis MJ, Kaban LB, Vacanti JP, Yelick PC. Tissue-engineered hybrid tooth and bone. Tissue Eng. 2005;11(9-10):1599–610.

74. Yoshikawa M, Tsuji N, Toda T, Ohgushi H. Osteogenic effect of hyaluronic acid sodium salt in the pores of a hydroxyapatite scaffold. Mater Sci Eng C. 2007;27(2):220–6.

75. Place ES, Evans ND, Stevens MM. Complexity in biomaterials for tissue engineering. Nat Mater.2009;8(6):457–70.

76. Huebsch N, Mooney DJ. Inspiration and application in the evolution of biomaterials. Nature. 2009;462:426–32.

77. Newman S, Tomasek JJ. Morphogenesis of connective tissues. Extracellular Matrices. Harwood Academic; 1996.

Chapter 3: Developmentally-Inspired Shrink-Wrap Polymers for Mechanical Induction of Tissue Differentiation

The following chapter is a reproduction of a paper I recently published in the journal Advanced Materials. It has been reproduced with permission.

Hashmi B, Zarzar L, Mammoto T, Mammoto A, Jiang A, Aizenberg J, and Ingber DE. Developmentally-Inspired Shrink-Wrap Polymers for Induction of Tissue Differentiation. *Adv. Materials* 2014; Feb 18 [Epub ahead of print].

Keywords: *scaffold engineering, biomaterials, odontogenesis, poly(N-isopropylacrylamide), thermoresponsive*

Local and abrupt changes in mechanical forces play a fundamental role in control of tissue and organ development. While some investigators have varied material properties of tissue engineering scaffolds to influence cell behavior, no biomaterials have been developed that harness mechanical actuation mechanisms to induce new tissue formation. Here, we describe the development of mechanically-actuatable polymers that induce tissue differentiation by harnessing the physical induction mechanism that drives tooth organ formation in the embryo. The formation of many epithelial organs is triggered when sparsely distributed mesenchymal cells abruptly pack closely together and undergo a “mesenchymal condensation“ response. For example, in tooth development, the associated physical compression and rounding of dental mesenchymal cells is sufficient to induce whole organ formation *in vitro* and *in vivo* [1]. Inspired by this developmental induction mechanism, we fabricated an artificial, shrink-wrap like polymer scaffold that can stimulate tooth tissue differentiation by abruptly inducing physical compaction of cells cultured within it when warmed to body temperature. A porous, GRGDS-modified, hydrogel scaffold was fabricated from poly(*N*-isopropylacrylamide) (PNIPAAm), which remains in an expanded form in the cold, and rapidly contracts volumetrically when placed at body temperature. When undifferentiated embryonic dental mesenchymal cells were seeded within this hydrogel sponge and polymer shrinkage was thermally induced by warming, the cells became physically compressed and exhibited a more compact, rounded morphology, as they do when they undergo mesenchymal condensation during tooth organ development in the embryo. This physical change in cell shape stimulated tooth differentiation, as measured by the induction of key odontogenic transcription factors *in vitro* and

stimulation of mineralization *in vivo*. This polymer-based mechanical actuation mechanism represents a new bioinspired approach to induce organ-specific tissue differentiation that could be useful for stem cell biology, tissue engineering and regenerative medicine.

Current design strategies used to fabricate materials for tissue engineering and regenerative medicine focus on the chemistry, structural properties, and three-dimensional (3D) spatial organization of the components that comprise these scaffolds (e.g., polymers, ceramics, biomaterials) [2,3]. While current tissue scaffold designs can support cell survival and maintenance of some differentiated cell functions, they do not exhibit the ability to induce major developmental lineage switches that can drive whole organ formation. Thus, we set out to develop materials that mimic the organ inductive properties of certain embryonic tissues. The formation of most organs in the embryo results from complex interactions between adjacent epithelial and mesenchymal tissues [4-7]. An initial instructive signal, provided by one of the tissue layers, is followed by reciprocal exchange of inductive signals, resulting in stepwise differentiation of both tissue components into an integrated organ structure. One of the simplest examples of organ formation is the development of the tooth. In the mouse, the embryonic day (E10) dental epithelium induces a ‘mesenchymal condensation’ response in which underlying mesenchymal cells are stimulated to migrate towards the base of the epithelium, resulting in formation of a tightly packed, dense cell aggregate in this region [1,8,9]. Recent studies have revealed that the physical compression of cells caused by this condensation response mechanically triggers the mesenchymal cells to express odontogenic (tooth forming) genes including Pax9, Msx1 and BMP4 [1,10,11].

Moreover, once induced in this manner, the mesenchyme can support whole tooth formation when recombined with normal embryonic dental epithelium and implanted under the kidney capsule in a mouse [1]. Importantly, similar mesenchymal condensation processes are crucial for the formation of many other epithelial organs, including the salivary gland, pancreas, kidney, bone, and cartilage among others [8,12-16], and thus, harnessing this induction mechanism could have much broader value for the field of tissue engineering.

Inspired by this mechanical organ induction mechanism, we set out to explore whether it is possible to develop artificial polymer scaffolds that can abruptly shrink in 3D, and thereby physically compress mesenchym cells cultured within the lattice to induce their differentiation. We designed a temperature-responsive polymer scaffold composed of poly(*N*-isopropylacrylamide) (PNIPAAm), which upon heating to physiological temperatures contracts in volume in 3D. PNIPAAm has been previously shown to autonomously change volume through alteration of temperature within physiologically relevant ranges [17-20]. The thermosensitivity of PNIPAAm is governed by its lower critical solution temperature (LCST): at temperatures below the LCST, the polymer is swollen, whereas it contracts when the polymer is heated to higher temperatures [21,22]. PNIPAAm's LCST also can be manipulated by adding other chemical moieties that change the hydrophilicity of the polymer, thereby allowing its thermoresponsiveness to be tailored for specific biological applications [17,19, 22]. Other parameters such as volume change, porosity, and biocompatibility also can be controlled by altering cross-linking density or adding adhesion-promoting components.

In the present study, we incorporated a GRGDS peptide into the cross-linked PNIPAAm polymer gel that mediates adhesion to cell surface integrin receptors in order to promote cell anchorage and survival [23-25]. The peptide was first modified with an acrylate moiety so that it could be polymerizable and then mixed into the hydrogel precursor solution containing 10% *N*-isopropylacrylamide (NIPAAm) monomer and 1% *N,N'*–methylenebisacrylamide (BIS) cross-linker by weight in water (Figure 3.1a).

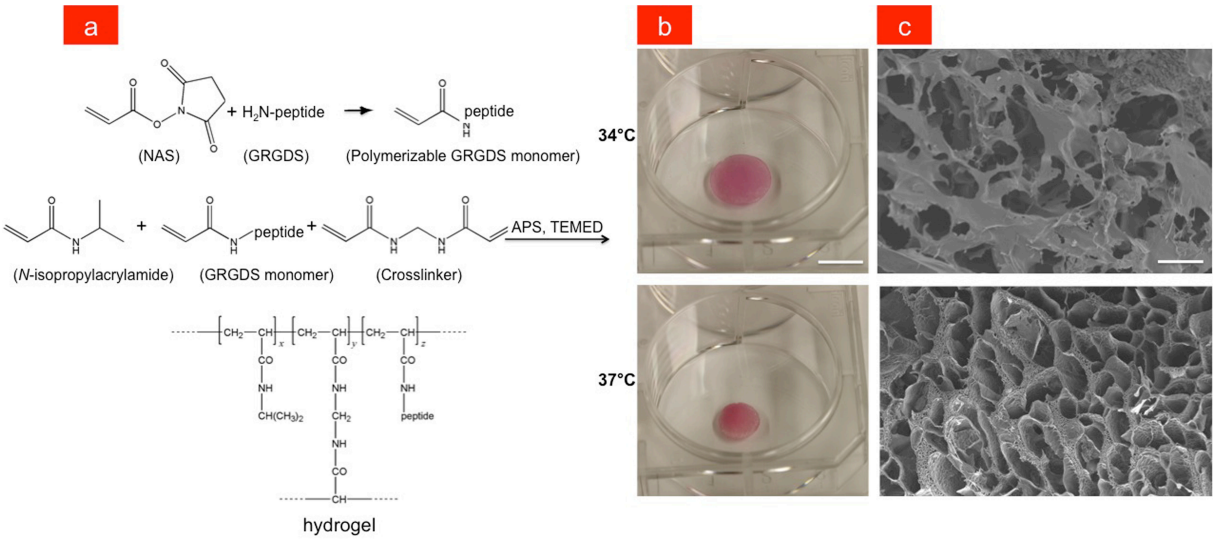

Figure 3.1 (a) Chemical synthesis of GRGDS-PNIPAAm. First the GRGDS peptide is modified with an acrylate moiety by reaction with *N*-acryloxysuccinimide (NAS) and is then mixed with a NIPAAm and BIS precursor solution. The hydrogel is then polymerized through radical initiation using APS and TEMED. (b) GRGDS-PNIPAAm in swollen and contracted states at 34°C and 37°C, respectively (bar, 1 cm). The red color arises from the hydrogel being submerged in serum-containing medium. (c) SEMs of GRGDS-PNIPAAm gels in swollen (top) and contracted (bottom state showing reduction in pore size with gel contraction (bar, 100 μm).

The hydrogel was polymerized by radical initiation using ammonium persulfate (APS) and tetramethylethylenediamine (TEMED), and then subsequently lyophilized (see Supporting Information for details). While PNIPAAm without peptide has an LCST of 32°C, the addition of even low concentrations of GRGDS significantly increased the LCST of the gel. For this reason, we experimentally determined the optimal concentration of peptide monomer necessary to yield hydrogels with an LCST of ~36°C, which is close to body temperature (Supplementary Figure S1). Swollen gels without cells were found to have an average pore size of 2398 + 211 μm and 1618 + 108 μm in their contracted state as determined from scanning electron micrographs of flash-frozen, lyophilized hydrogels, and these hydrogels contracted volumetrically by approximately 45% when heated from 34°C to 37°C in medium containing 10% fetal bovine serum (Figure 3.1b-c). The volumetric response was also reversible in that GRGDS-PNIPAAm gels that contracted at 37°C could be induced to swell back to their original size by lowering the temperature.

To determine whether cells cultured within the temperature-responsive scaffolds could be physically compressed by inducing gel shrinkage, dental mesenchymal cells originally isolated from E10 mouse embryos were implanted within the GRGDS-modified PNIPAAm gel, cultured overnight at 34°C, and then either maintained at the same temperature or shifted to 37°C for 48 hours. Importantly, while cells maintained at the lower temperature exhibited polygonal cell morphology (Figure 3.2a) similar to that observed on conventional culture substrates, these cells formed tighly compacted, dense aggregates and exhibited a round morphology when the the hydrogel was induced to shrink by raising the temperature to 37°C (Figure 3.2a-c). Computerized

morphometric analysis confirmed that projected cell areas reduced by more than 60% when this compression response was mechanically triggered (Figure 3.2c), which is similar to the rounding and reduction in cell size that was shown to be sufficient to induce these dental mesenchymal cells to undergo odontogenic differentiation *in vitro* and *in vivo* [1].

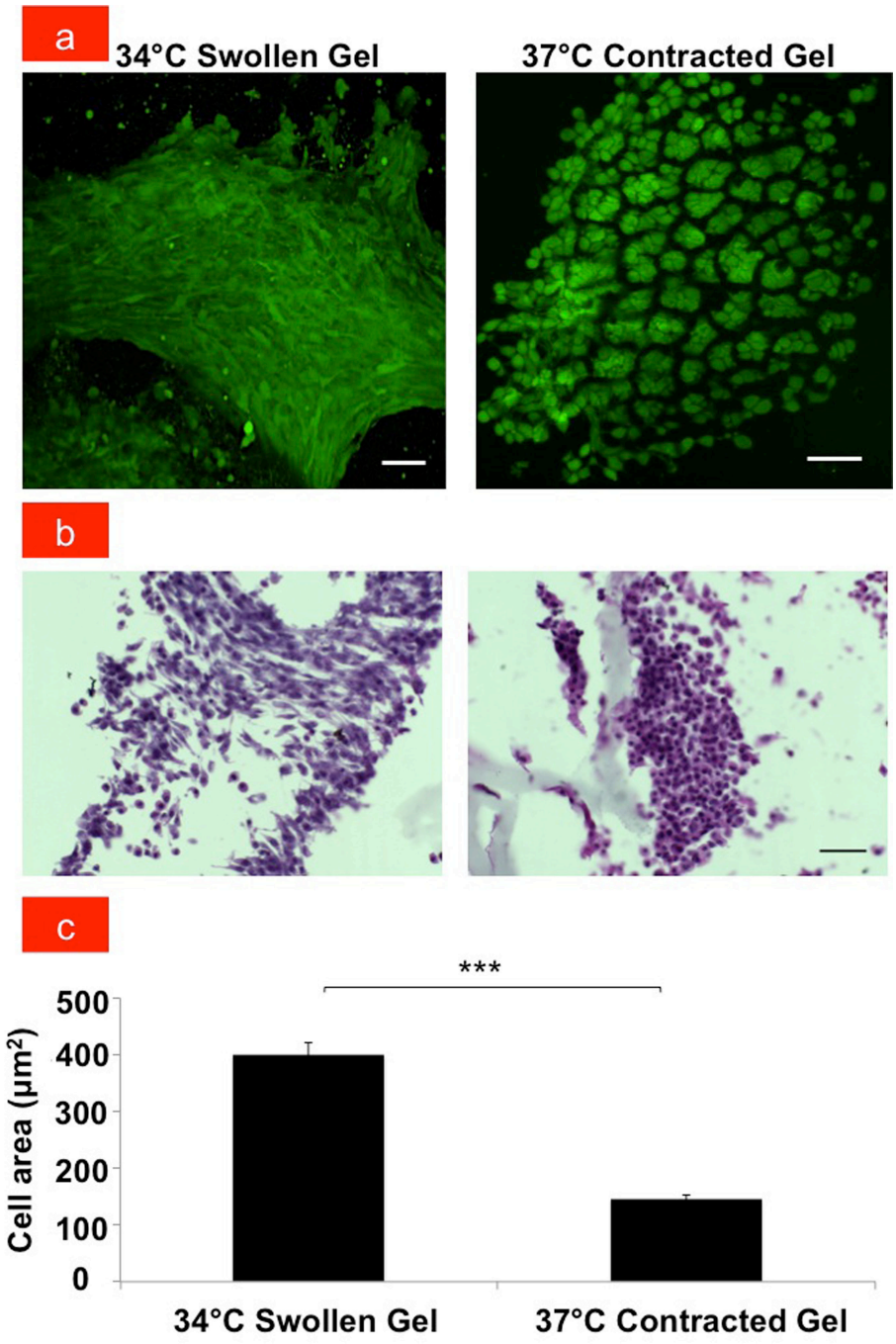

Figure 3.2 (a) Fluorescent micrographs of E10 dental mesenchymal cells in swollen GRGDS-PNIPAAm hydrogel at 34°C and in contracted GRGDS-PNIPAAm hydrogel at 37°C (bar, 50 μm). (b) Light micrographs showing hematoxylin and eosin (H&E)

Figure 3.2 (Continued)…staining of mesenchymal cells that appear spread in the swollen GRGDS-PNIPAAm hydrogel, where as they are compact and rounded in the contracted GRGDS-PNIPAAm hydrogel at 37°C (bar, 50 μm). (c) Graph showing the quantification of the corresponding projected cell areas; ***p<0.001.

Moreover, time-lapse 2D and 3D imaging of the same gel revealed that cell rounding response occurred in parallel with gel contraction and that this occurred rapidly (< 15 min) after the temperature was raised (Supplementary Videos V1 and V2, respectively), thus, confirming that this a direct effect of mechanical compaction. Although the rate of the cell shape change varies depending on how quickly the heating chamber of the microscope equilibrated to the warmer temperature, the cell volume decreased at approximately $1.64x10^5$ μm^3/min in our 3D time-lapse study (Supplementary Figure S2). Importantly, most of the cells cultured at 37^oC in the contracted GRGDS-gels remained viable for at least two weeks in culture as determined by cell viability, cytotoxicity, and growth assays, whereas cells on PNIPAAm gels without GRGDS rapidly lost their viability with virtually all cells dying within the first week (Supplementary Figures S3 & S4).

Next, we explored whether the cell shape change and compaction induced by the hydrogel compression influenced expression of three different genes that are critical drivers of tooth formation - Pax9, Msx1, and Bmp4 [1,26,27]. Immunofluorescence staining for Pax9 protein confirmed that increased numbers of cells expressed this odontogenic transcription factor when cultured in contracted gels placed at 37°C that induced cell rounding compared to swollen gels maintained at the lower temperature

where no compaction was observed (Figure 3.3a). Similar responses were observed when we used PCR to quantitate changes in mRNA levels for Pax9 as well as for two other genes – Msx1 and Bmp4 – that are also key drivers of tooth formation [1,26,27] (Figure 3.3b).

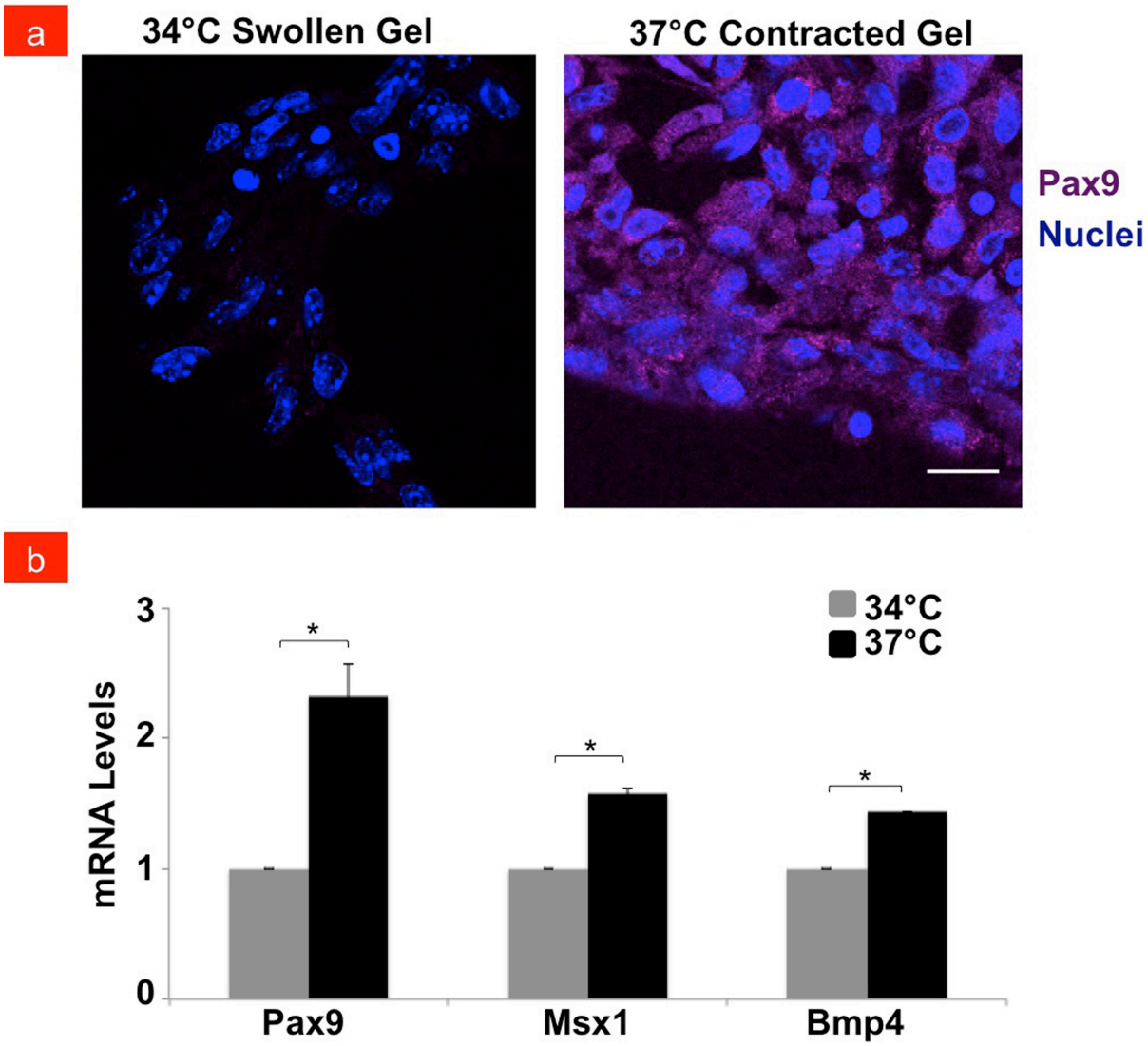

Figure 3.3 Fluorescent micrographs showing (a) Pax9 protein expression (purple) in mesenchymal cells with their nuclei stained with DAPI (blue) cultured in swollen versus contracted gels at 34°C or 37°C, respectively (bar, 20 μm). Pax9 expression is noted in contracted gels and absent in swollen gels. (b) Graph showing the quantification of

Figure 3.3 (Continued)…mRNA expression levels of Pax9, Msx1 and Bmp4 odontogenic markers in compacted mesenchymal cells within contracted PNIPAAm gels. mRNA levels in cells cultured at 37°C (black bars) are shown relative to 34°C controls (grey bars); *p<0.05.

Pax9 mRNA levels doubled in contracted gels relative to cells in gels maintained at 34°C, and Msx1 and Bmp4 increased by ~1.5-fold within 2 days after stimulation from hydrogel contraction (p<0.05). Expression of these odontogenic markers was not affected by these temperature differences alone as confirmed by control experiments with cells cultured at 34°C and 37°C under standard culture conditions (Supplementary Figure S5).

The long-range goal of this effort is to design and fabricate biomimetic inductive scaffolds developmental induction for *in vivo* tissue engineering. To begin to explore the feasibility of this approach, GRGDS-PNIPAAm gels seeded with $1x10^6$ dental mesenchymal cells were implanted under the kidney capsule of an adult mouse using a published method for *in vivo* analysis of tooth formation (Figure 3.4a & Supplementary Figure S6) [1,28]. As these gels spontaneously contract when placed at body temperature, a cell pellet containing the same number of cells without a scaffold was implanted as a control. Additional *in vivo* controls included implantation of the GRGDS-PNIPAAm gel alone without DM cells and use of a GRGDS-PNIPAAm gel designed with an LCST above 37°C containing the same number of DM cells.

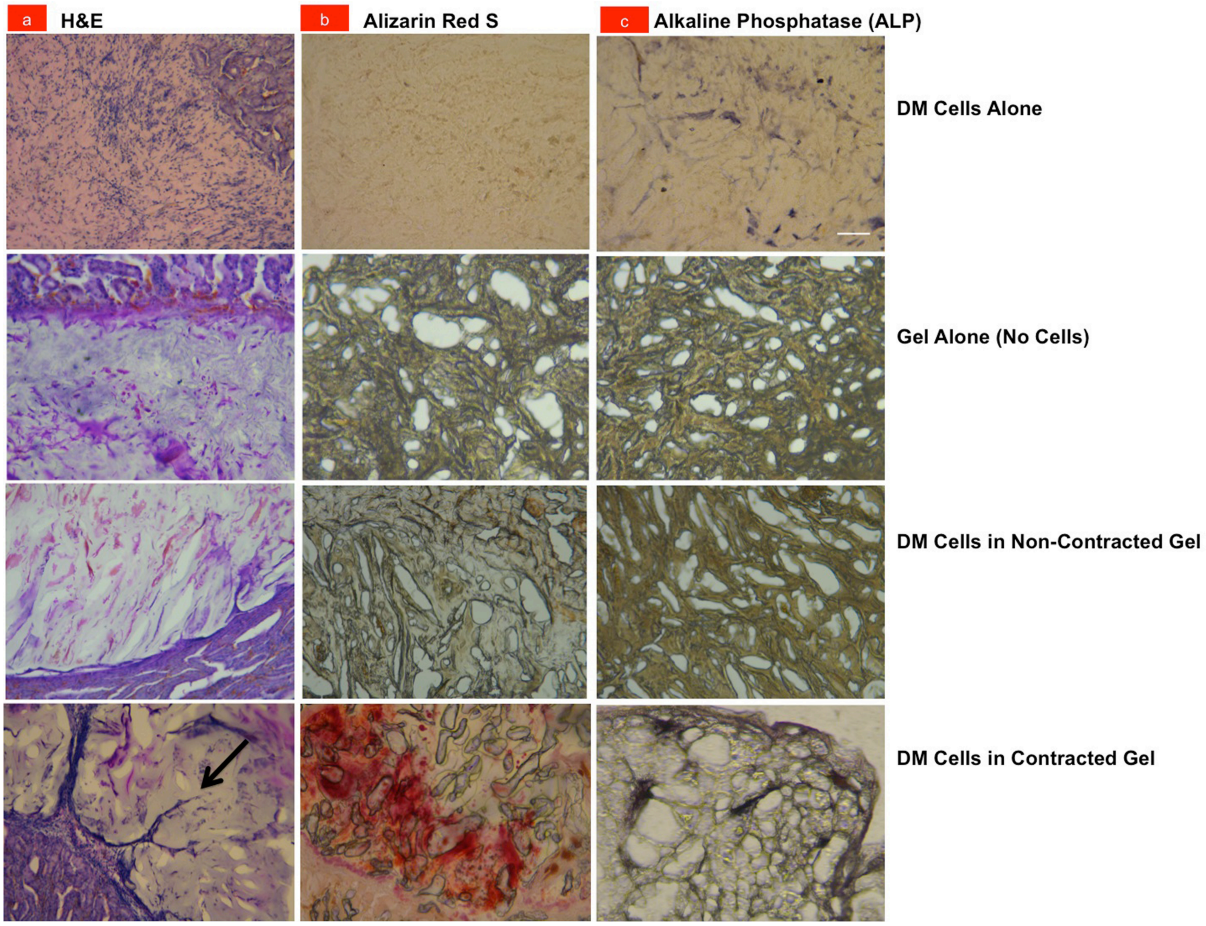

Figure 3.4 Light micrographs of histological sections of the control dental mesenchymal (DM) cell pellet alone (DM Cells Alone), GRGDS-PNIPAAm gel without cells (Gel Alone/No Cells), DM cells in a non-contracted gel with a LCST>37°C (DM Cells in Non-Contracted Gel), and a contracted GRGDS-PNIPAAm gel containing DM cells (DM Cells in Contracted Gel) when implanted for 2 weeks under the kidney capsule of a mouse. Sections were stained with (a) Hematoxylin and eosin (H&E) or (b) Alizarin Red S, or analyzed for (c) Alkaline Phosphatase (ALP) activity; arrow indicates a new capillary sprout (bar, 100 μm).

Histological analysis of these implants after 2 weeks revealed that only the contracted gel containing cells implanted within the shrink wrap GRGDS-PNIPAAm polymer induced neovascularization (Figure 3.4a), and physical compaction of the DM cells could be detected *in vivo* (Supplementary Figure S7). Staining with Alizarin Red S and alkaline phosphatase (ALP) revealed that only the implants containing cells within contracted GRGDS-PNIPAAm gels were positive for deposition of calcium and mineralization, respectively (Figure 3.4b-c), which are indicative of later stages of tooth formation [1,16,27,28]. In contrast, neither mineralization nor vascularization was observed when the cell pellet or gel was implanted alone, or when the higher LCST gel (that did not contract at 37°C) with DM cells was implanted (Fig. 3.4b-c). Taken together, these results clearly demonstrate that mechanical compression of DM cells within the contracting gel was required fort he induction of the mineralization and vascularization we observed.

These findings confirm that a developmentally-inspired biomimetic scaffold that induces mesenchymal condensation mechanically can potentially be used to therapeutically stimulate cell and tissue differentiation *in vitro* as well as *in vivo*. In past studies, we showed that physical compression of cells during the mesenchymal condensation process is the key signal that triggers tooth formation, and that this is mediated by cell shape-dependent changes in the expression of two key odontogenic transcription factors (Pax9 and Msx1) and one important morphogen (Bmp4) [1]. The results of the present study confirm that physical compaction of dental mesenchymal cells is indeed the key regulator of this tooth differentiation pathway. Responsive polymers have been previously used for controlled release of drugs and cells [19,29],

and PNIPAAm has been employed to control cell adhesion and release tissues from substrates after they have formed [30]. But to our knowledge, this is the first study demonstrating the use of a responsive polymer, such as PNIPAAm, to induce tissue differentiation specifically by mechanically actuating a cell compaction response. It is also the first to promote tissue engineering by mimicking a developmental organ induction response.

We only focused on the effects of polymer shrinkage-induced compression of dental mesenchymal cells on tissue differentiation in the present study because inclusion of dental epithelial cells would have complicated our analysis. However, previous work has shown that induced dental mesenchymal cells must be recombined with dental epithelial cells in order to produce fully formed teeth *in vivo*. [1,28] Thus, tissue recombination studies should be explored in the future to fully define the value of this approach for organ engineering applications.

Many other organs require mesenchymal condensation for their induction and formation, including salivary gland, pancreas, kidney, bone, and cartilage, [12-16] and so these inductive polymer gels could have value for engineering of many tissues. Mechanically actuating polymer systems potentially could be used to suppress cancer growth as past studies have shown that tumor expansion can be accelerated or suppressed by altering tissue mechanics and cell distortion [31,32]. Thus, this shrink wrap polymer strategy will likely have broad applications for tissue engineering, regenerative medicine, and clinical therapy as well as value for basic research aimed at understanding and manipulating organ formation and regeneration.

Experimental Methods

Experimental System: Our methods for separation of dental mesenchyme from dental epithelium of embryonic mouse mandible have been published [1]. In brief, embryos were removed from timed pregnant CD1 mice at E10 and the molar tooth germ was microdissected free under a dissecting microscope. To separate the dental mesenchyme from the epithelium, the tissues were incubated with Dispase (2.4U/ml) with DNase in Ca^{2+}-Mg^{2+} free PBS for 20-30 min at 37°C [1]. The tissues were then washed in 10% FBS DMEM, and the epithelium was mechanically pulled free from the dental mesenchyme using fine forceps. Cells from remaining E10 dental mesenchyme were cultured in 10% FBS DMEM in T-75 tissue culture flasks, with medium changed every 2-3 days; all studies were carried with dental mesenchymal cells that were cultured for less than 12 passages.

Hydrogel Fabrication: N-acryloxysuccinimide (NAS), *N*-isopropylacrylamide (NIPAAm), and *N,N'*-methylenebisacrylamide (BIS) were purchased from Sigma Aldrich; ammonium persulfate (APS) was purchased from Mallinckrodt; tetramethylethylenediamine (TEMED) was purchased from Calbiochem, sodium bicarbonate was purchased from Sigma Aldrich, and GRGDS peptide was purchased from Bachem Biosciences. All were used as received except for the NIPAAm, which was recrystallized from hexane.

The lyophilized acrylate-modified GRGDS was redistributed in hydrogel precursor (10% NIPAAm, 1% BIS w/v in deionized water). The concentration used was determined experimentally to produce gels with a desired LCST ≈36°C. To make a hydrogel scaffold, the peptide/gel precursor (50 µL) was placed in the (1 cm) diameter

well of a MatTek glass bottom dish, then aqueous APS solution (4 µL, 10% w/v) was added, followed by TEMED (0.5 µL) and stirring. Gelation occurred within a minute. Gels were transferred to a water bath where they were left for 3 days at 4°C to allow any unreacted monomers and initiators to diffuse out of the gel. Each hydrogel was then transferred individually to a centrifuge tube (15 mL) filled partially with water, frozen (-80°C), and lyophilized. Hydrogel characterization was carried out using differential scanning calorimetry (TA Instruments DSC Q200) and the LCST was determined to be ≈36°C. For fabrication of gels with a LCST greater than 37°C, the same protocol was followed, except that the concentration of GRGDS peptide was doubled. Scans were performed at a rate of (5°C/min). For scanning electron microscopy (SEM), dry samples were sputter coated with Au/Pd prior to imaging on a JEOL JSM 639OLV SEM.

Peptide Modification: GRGDS was modified with an acrylate moiety on the N-terminus to allow copolymerization into the hydrogel scaffolds. GRGDS (6.25 mg) was dissolved in (6 mL) sodium bicarbonate buffer (pH=8.2) and stirred in a round bottom flask while a solution of NAS (0.02g NAS in 3 mL of sodium bicarbonate buffer) was added dropwise. The solution was stirred in the dark for 2.5 hours at room temperature. The solution was dialyzed for 3 days at 4°C against deionized water with frequent bath changes to remove unreacted NAS (Spectra/Por Float-A-Lyzer G2, 10 mL, 0.1-0.5 kD MWCO cellulose ester membrane) and the product was lyophilized.

Cell Seeding: Upon polymerization, the GRGDS-PNIPAAm gels were sterilized by being washed with 70% Ethanol-PBS, PBS, and then subsequently submerged in 10% FBS-DMEM at 25°C. Dental mesenchymal cells were then trypsinized and injected in the hydrogel using a (25 guage) syringe needle at room temperature. The hydrogels with

the injected cells were placed overnight in a 34°C incubator under 5% CO_2 to allow for cell adhesion to occur. These hydrogels were then subsequently shifted to a 37°C incubator under 5% CO_2 to induce their contraction. They were maintained under these conditions overnight for *in vitro* quantitative PCR assays and a period of 1-3 weeks for cell viability assays and fluorescence imaging.

Functional Assays: Cells in PNIPAAm hydrogels were stained using the Live/Dead Viability/Cytotoxicity Kit for mammalian cells (Invitrogen) according to protocols provided.

For Alkaline Phosphatase (ALP) activity and Alizarin Red S staining, cryosectioned samples on slides were rinsed with calcium and magnesium negative Phosphate Buffer Solution (PBS, Gibco Life Technologies) three times. Samples were then covered in 5-Bromo-4-chloro-3-indolyl Phosphate/Nitroblue Tetrazolium (BCIP/NBT) Liquid Substrate (0.692 mM/L BCIP; 0.734 mM/L NBT) (MP Biomedicals LLC) solution for ALP staining, or in Alizarin Red S powder (20 mg, Sigma Aldrich) mixed with deionized water (20 mL) and adjusted to (pH 6.3). Samples were then rinsed with PBS three times again prior to subsequent mounting and imaging

Quantitative PCR: Quantitative PCR was performed to analyze changes in expression levels of key odontogenic regulatory molecules, as previously described [1]. Pax9 antibodies also were purchased from Abcam (Cambridge MA) and corresponding secondary antibody from Invitrogen (Life Technologies).

Sectioning, Analyses, Imaging: Our methods for cryosectioning, histological analysis, hematoxylin and eosin (H&E) staining, immunohistochemistry (IHC), confocal microscopy, fluorescent miscroscopy, computerized image analysis have been

previously published [1-4]. Anti-Ki-67 antibody was purchased from Abcam (Cambridge MA) and corresponding secondary antibody from Invitrogen (Life Technologies). In brief, an inverted laser scanning confocal microscope (Leica SP5XMP, Buffalo Grove, IL, USA) with acquisition of multiple z-stack sections as well as an inverted fluorescent microscope (Zeiss Axio Observer Z12) with z-stack sections and color camera microscope (Zeiss Axio Zoom V16) were used for imaging and aquisition of time-lapse videos. ImageJ software (NIH Bethesda MD) was used for cell area morphometric analysis. Bitplane Imaris 7.6 F1with Huygens Deconvolution software was used to 3D render the confocal microscope time-lapse and cell volumetric images over time.

Animal Experiments: All animal studies were approved by the Animal Care and Use Committee of Children's Hospital Boston. For *in vivo* experiments, gels placed in a 34°C incubator under 5% CO_2 overnight were implanted under the kidney capsule [5,6] and histological analyses were performed 14 days after the implantation, as previously described [1].

Statistical Analyses: Students' t-test was used for cell size (projected cell area) comparison and qPCR results. Results are presented in mean +/- the standard error of the mean unless otherwise stated.

References from Experimental Section

[1] T. Mammoto, A. Mammoto, Y. S. Torisawa, T. Tat, A. Gibbs, R. Derda, R. Mannix, M. de Bruijn, C. W. Yung, D.Huh, D. E. Ingber, *Dev. Cell* **2011**, *21*, 758-69.

[2] C. S. Chen, M. Mrksich, S. Huang, G. M. Whitesides, D. E. Ingber, Science **1997,** 276, 1425-1428.

[3] Y. Numaguchi, S. Huang, T. R. Polte, G. S. Eichler, N. Wang, D. E. Ingber, *Angiogenesis* **2003**, 6, 55-64.

[4] T. Mammoto, A. Jiang, E. Jiang, D. Panigrahy, M.W. Kieran, A. Mammoto, *Am J Pathol* **2013**, 183, 1293-305.

[5] A. Ohazama, S. A. Modino, I. Miletich, P. T. Sharpe, J. Dent. Res. **2004**, 83, 518-22.

[6] K. Nakao, R. Morita, Y. Saji, K. Ishida, Y. Tomita, M. Ogawa, M. Saitoh, Y. Tomooka, T. Tsuji, Nat. Methods **2004**, 4, 227-30.

Acknowledgements

This work was conducted with support by grants from the NIH Common Fund (RL1DE019023 to D.E.I.), the Wyss Institute for Biologically Inspired Engineering at Harvard University, and partially from the DOE BES (DE-SC0005247 to J.A.). We would like to thank E. Jiang and M. Kowalski for their technical assistance and T. Ferrante for assistance in imaging.

References:

[1] T. Mammoto, A. Mammoto, Y. S. Torisawa, T. Tat, A. Gibbs, R. Derda, R. Mannix, M. de Bruijn, C. W. Yung, D.Huh, D. E. Ingber, *Dev. Cell* **2011**, *21*, 758-69.

[2] E. S. Place, N. D. Evans, M. M. Stevens, *Nat. Mater.* **2009,** *8***,** 457-70.

[3] N. Huebsch, D. J. Mooney, *Nature* **2009**, *462*, 426-32.

[4] A. G. Jacobson, *Science* **1966**, *152*, 25-34.

[5] C. Grobstein, *Natl. Cancer Inst. Monogr.* **1967**, *26*, 279-99.

[6] M. Bernfield, S. D. Banerjee, J. E. Koda, A. C. Rapraeger, *Ciba Found. Symp.* **1984**, *108*, 179-96.

[7] J. B. Gurdon, *Development* **1987**, *99*, 285-306.

[8] L. Saxén, I. Thesleff, *Ciba Found. Symp.* **1992**, *165*, 183-92.

[9] J. Jernvall, I. Thesleff, *Mech. Dev.* **2000**, *92*, 19-29.

[10] M. Mina, E. J. Kollar, *Arch. Oral Biol.* **1987**, *32*, 123-7.

[11] M. Bei, K. Kratochwil, R. L. Maas, *Development* **2000**, *127*, 4711-8.

[12] C. Grobstein, *Nature* **1953***, 172*, 869-70.

[13] N. Golosow, C. Grobstein, *Dev. Biol.* **1962**, *4*, 242-55.

[14] M. M. Smith, B. K. Hall, *Biol. Rev. Camb. Philos. Soc.* **1990**, *65*, 277-373.

[15] B. K. Hall, T. Miyake, *Anat. Embryol.* **1992**, *186*, 107-24.

[16] I. Thesleff, A. Vaahtokari, A. M. Partanen, *Int. J. Dev. Biol.* **1995**, *39*, 35-50.

[17] H. Tekin, M. Anaya, M. Brigham, C. Nauman, R. Langer, A. Khademhosseini, *Lab Chip* **2010**, *10*, 2411-18.

[18] H. Tekin, J. G. Sanchez, C. Landeros, K. Dubbin, R. Langer, A. Khademhosseini, *Adv. Mater.* **2012**, *24*, 5543-47.

[19] L. Klouda, K. R. Perkins, B. M. Watson, M. C. Hacker, S. J. Bryant, R. M. Raphael, F. K. Kasper, A. G. Mikos, *Acta Biomater*. **2011**, *7*, 1460-7.

[20] D. Schmaljohann, *Adv. Drug Deliv. Rev.* **2006**, *58*, 1655-70.

[21] H. G. Schild, *Prog. Polym. Sci*. **1992**, *17,* 163-249.

[22] L. Klouda, A. G. Mikos, *Eur. J. Pharm. Biopharm.* **2008**, *68*, 34-45.

[23] D. L. Hern, J. A. Hubbell, *J. Biomed. Mater. Res.* **1998**, *39*, 266-76.

[24] U. Hersel, C. Dahmen, H. Kessler, *Biomaterials* **2003**, *24*, 4385-415.

[25] X. B. Yang, H. I. Roach, N. M. P. Clarke, S. M. Howdle, R. Quirk, K. M. Shakesheff, R. O. C. Oreffo, *Bone* **2001**, *29*, 523-31.

[26] I. Thesleff, *Acta Odontol. Scand.* **1998**, *56*, 321-5.

[27] I. Thesleff, *J. Cell Sci.* **2003**, *116*, 1647-48.

[28] A. Ohazama, S. A. Modino, I. Miletich, P. T. Sharpe, J. Dent. Res. **2004**, 83, 518-22.

[29] X. Zhao, J. Kim, C. A. Cezar, N. Huebsch, K. Lee, K. Bouhadir, D. J. Mooney, *Proc. Natl. Acad. Sci. U.S.A* **2011**, *108*, 67-72.

[30] H. Takahashi, N. Matsuzaka, M. Nakayama, A. Kikuchi, M. Yamato, T. Okano, *Biomacromolecules* **2012,** *13*, 253-60.

[31] K. R. Levental, H. Yu, L. Kass, J. N. Lakins, M. Egeblad, J. T. Erler, S. F. Fong, K. Csiszar, A. Giaccia, W. Weninger, M. Yamauchi, D. L. Gasser, V. M. Weaver, *Cell*

2009, *139*, 891-906.

[32] M. J. Paszek, V. M. Weaver, *J. Mammary Gland Biol. Neoplasia* **2004**, *9*, 325-42.

Chapter 4: A Combinatorial Mechanochemical Microarray for Identification of Differentiation-Inducing Extracellular Matrix Materials

The following chapter describes a soon to be submitted study I have done in colloboration with Keekyoung Kim, Jalil Zerdani, Ali Khaddemhosseini and Donald E. Ingber of which I am the lead author.

Abstract

Microarray printing technologies have been adapted for tissue engineering applications to screen for synthetic polymers or ECM components that exhibit enhanced differentiation-inducing properties. Similar approaches have been used to screen for differences in substrate mechanical properties that differ in their differentiation-inducing behavior; however, the stiffness range explored was limited to more rigid domains that are not relevant for engineering of many cells, such as stem cells and embryonic mesenchymal cells. Here, we describe the development of a polyacrylamide (PAA) gel microarray platform created with a robotic spotting machine that permits analysis of cell behavior when adherent to ECM islands with defined chemistry and a more physiologically relevant range of mechanical compliance than described previously. To demonstrate proof-of-principle, we used this combinatorial screening method to determine the effects of various combinations of different ECM formulations (collagen VI and tenascin at different concentrations, alone or combined) and substrate stiffnesses (~130 to 1500 Pa) on induction of tooth differentiation in cultured embryonic mesenchymal cells. These studies revealed that the stiffest ECM islands with the lowest collagen VI coating density

induced a higher degree of tooth differentiation than the other material combinations tested, and that tenascin was much less effective on the flexible ECM islands than when coated on a rigid glass substrate. This screening platform may be useful for the selection of tooth-inducing biomaterials, and more generally, for identification of materials that produce desired effects on cell differentiation or function based on their unique mechanical and chemical properties.

Keywords: *extracellular matrix, microarray, combinatorial screening, mechanics, polyacrylamide gel, differentiation, tooth*

Introduction

Microarray printing technologies initially developed for genome-wide gene profiling have been adapted for tissue engineering applications by depositing multiplexed arrays of different synthetic polymers or extracellular matrix (ECM) molecules, making it possible to identify biomaterials that have enhanced abilities to promote cell differentiation or direct stem cell fates [1–5]. Development of synthetic scaffolds for tissue engineered initially focused on optimization of the chemical composition, spatial arrangement and biodegradability of these materials, while providing appropriate ECM ligands to support cell adhesion and function [6,7]. However, mechanical forces conveyed to cells through their ECM adhesions contribute significantly to control of tissue and organ development in the embryo, as well as tissue regeneration during wound healing [8]. This has led to development of synthetic biomaterials for tissue engineering with unique mechanical properties designed to improve formation of specialized tissues. For example, ECM substrates with different mechanical properties have been fabricated and shown to produce stiffness-specific effects on cell functions (e.g., motility, growth, contractility), stem cell differentiation, and angiogenesis [8–11]. But mechanical and chemical cues interplay in a complex manner during development because cells sense these signals simultaneously in the living tissue microenvironment, and changes in ECM mechanics that alter cell shape and tension regulate cell fate switching by modulating sensitivity to both adhesive signals and soluble factors [12–14].

The effects of ECM microenvironments have been explored using microarray printing technology due to its economic benefit in preserving time, volume of

materials being utilized, and producing results efficiently [15]. Others have utilized this system to determine the mechanical properties of a large biomaterials library[16]. However, current printing technologies are limited in terms of their ability to print soft mechanical substrates that are required for studies of induction[17–19], and it has been difficult to vary ECM type, density and mechanics in the same microarray printed materials. For example, in studies with microspotted islands of fibronectin, the most flexible islands fabricated were in the kPa range [5], which is an order of magnitude greater than the stiffness of natural living tissues such as the mammary gland, brain, liver, etc [20].

Thus, we set out here to develop a system that could microprint ECM islands of defined chemistry and greater mechanical compliance, and we focused on engineering materials that could mimic embryonic induction events as a proof-of-principle. We focused on embryonic tooth formation (odontogenesis) as a model system because recent work has identified that organ induction is controlled mechanically in this system [21,22], and there are good markers of tooth differentiation, such as expression of the odontogenic transcription factor Pax9 [21–24]. Two ECM proteins known to be present in the condensed mesenchyme during tooth development at the onset of epithelial budding, Collagen VI and tenascin, also have been suggested to play an important role in the tooth formation process [21,25–27]. This model is also clinically relevant because hypodontia, which is associated with early tooth loss or agenesis, is a significant problem in children where it is difficult to obtain stable dental implants due to active jaw growth [28–30].

Materials and Methods

ECM Microarray Preparation

Standard microscope 25 x 75 mm glass slides (Thermo Fisher Scientific, Waltham, MA) cleaned with concentrated sodium hydroxide solution to produce a smooth, residue free glass surface were dried and coated with 3-(trimethoxysilyl) propyl methacrylate (TMSPMA) (Sigma-Aldrich, St. Louis, MO) at 80°C overnight to provide a hydrophobic methacrylate-functionalized surface. To create a thin PAA pad (500 μm), a drop (167 ul) of liquid PAA solution [40% acrylamide (BioRad, Hercules, CA), 2% bisacrylamide (BioRad, Hercules, CA) in varying ratios [31,32] along with the free radical initiators, 50 ug/ml of 10% ammonium persulfate (Sigma-Aldrich, St. Louis, MO) and 5 ug/ml TEMED (BioRad, Hercules, CA) was placed on the methacrylated glass slide and a 18 mm by 18 mm plastic cover slip was placed on top. The ratios of 40% acrylamide/2% bisacrylamide were 1:0.1, 1:0.25, 1:1.25 for 132 Pa, 558 Pa and 1510 Pa, respectively. A single glass slide contained all 3 substrates (132 Pa, 558 Pa, 1510 Pa) in 3 different regions marked by the 18 mm by 18 mm coverslip as shown in Figure 4.1.

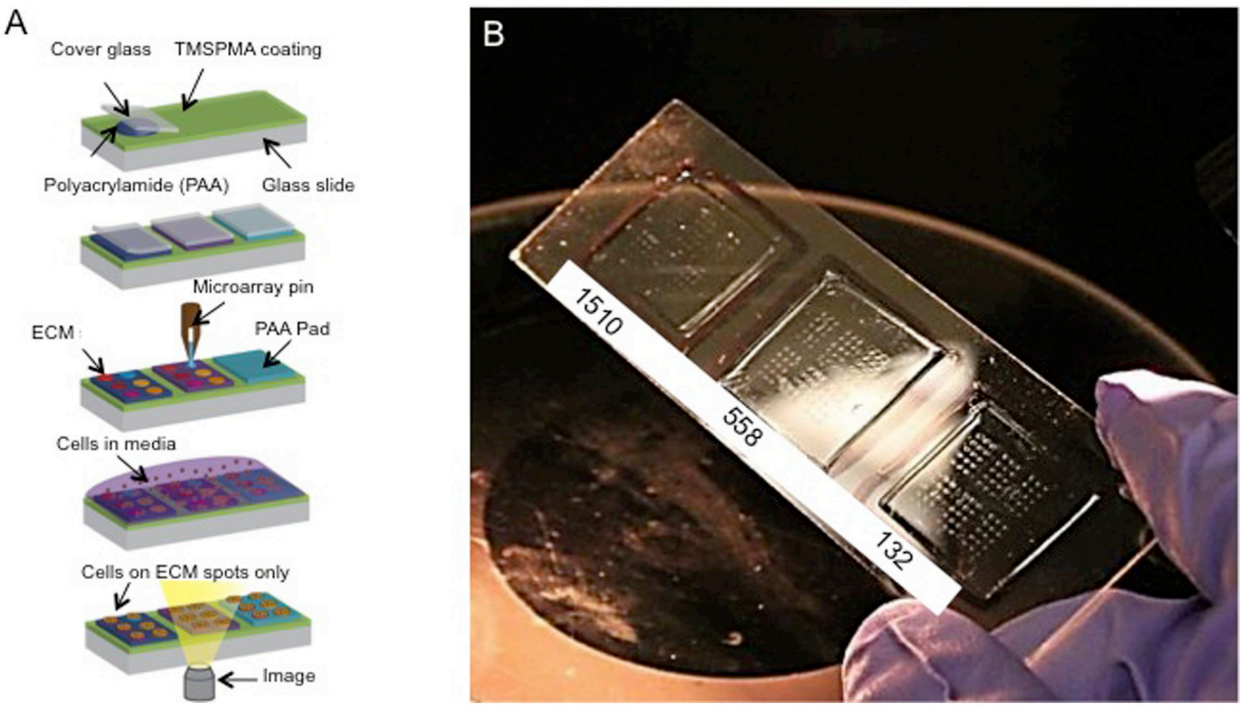

*3-(trimethoxysilyl) propyl methacrylate

Figure 4.1 Schematic and overview of microarray printing on PAA gel pads. (A) Schematic of printing protocol of stiffness dependent substrate. (B) Macro image of printed spots on a standard 25 mm x 75 mm glass slide with acrylamide gel pad substrate at 1510, 558, and 132 Pa. 15 replicate spots/slide for each condition were printed and 4 microarray data sets analyzed.

The glass slides were left overnight in a controlled humidity condition and subsequently the cover slip was peeled off from the polymerized gels in distilled deionized water. The PAA gel pads were then allowed to dry at room temperature before microarray printing.

ECM proteins were printed on the top surface of the PAA gels with a 2-pin contact microarray printer (SpotBot 3 Personal Microarray, ArrayIt,CA). The ink

used for printing contained either 100, 200 or 300 μg/ml of collagen VI (Abcam), 10 μg/ml tenascin (EMD Millipore), or a mixture of both, diluted in bovine serum and printing buffer. Bovine serum albumin (BSA; Sigma-Aldrich) was included in the solution to maintain the total amount of protein constant (24 ug) in all inks at a total volume of 80 ul per ECM protein biomaterial library. Each slide contained 90 individual spots, with 15 replicates for each of the 6 experimental conditions and 60 replicates for each condition. The printing buffer consisted of 20% glycerol (VWR), 5 mM EDTA (VWR), 100mM acetic acid (VWR), and 0.25% Triton X-100 (BioRad, Hercules, CA) at pH 5.0 to prevent protein polymerization [2]. The printing pins also were sonicated for 30 minutes in a 50% ethanol-water solution prior to printing, and the pins were washed in a 50% DMSO-water solution, rinsed in with distilled deionized water, and dried after printing each set of samples to ensure unrestricted flow. After printing, the glass slides were incubated for 8-16 hours at 4°C, and then washed 3 times with PBS to rehydrate the PAA gel pads prior to cell seeding.

Cells were plated on the microarray ECM spots at a density of 5.5×10^4 cells/cm^2 in DMEM containing 2% FBS, cultured overnight, and then fixed in 4% paraformaldehyde (PFA, BioRad, Hercules, CA) in PBS the next day for immunofluorescence microscopic analysis of cell morphology and differentiation.

Mechanical Characterization

The stiffness (shear and storage moduli) of arylamide gel substrates fabricated with different degrees of chemical cross-linking were characterized using a 8 mm plate geometry configuration in a Rheometer (AR-G2 TA instruments, DE). The minimum oscillation normal force limit was set to 0.1 N and maximum oscillation

normal force limit was 50 N; angular frequency was held constant at 6.283 rad/s and all studies were carried out at 25°C.

Cell Culture

Embryonic stage 10 murine mandibular mesenchymal (MM) cells transfected with green fluorescent protein (GFP) were used in all studies. MM cell suspensions were added to pre-warmed Dulbecco's modified Eagle's medium (DMEM, Gibco, Carlsbad, CA) supplemented with 10% fetal bovine serum (FBS, Invitrogen, Carlsbad, CA) and and 1% penicillin/streptomyocin, (Gibco, Carlsbad, CA), centrifuged at 1000 rpm, resuspended in culture medium, transferred to T75 tissue culture flasks (BD Biosciences, San Jose, CA), and cultured at 37°C under 5% CO_2. Cell cultures were refed with new medium every 2-3 days, and cells were passaged using 0.05% EDTA-trypsin (Invitrogen, Carlsbad, CA) when confluency was ~90%; all studies were carried out using cells prior to passage 12.

Immunohistochemistry

ECM microarrays with adherent cells were fixed, rinsed with PBS, permeabilized with 0.1% TritonX-100 (BioRad, Hercules, CA, USA) in PBS, and then incubated in 0.1% TritonX-100 containing 10% FBS in PBS for 1 hour prior to carrying out immunostaining using an antibody directed against rat pax 9 (1:100 dilution; Abcam, Cambridge, MA, USA) followed by incubation with an Alexa Fluor 594 conjugated anti-rat secondary antibody (1:200; Abcam, Cambridge, MA, USA) at room temperature. Upon completion, slides were dip coated with immunofluorescence mounting medium containing DAPI to visualize nuclei prior to placing the coverslip. Microarray spots and adherent cells were imaged using an inverted laser scanning

confocal microscope (Leica SP5XMP, Buffalo Grove, IL, USA) with acquisition of multiple z-stack sections as well as an inverted fluorescent microscope (Zeiss Axio Observer Z12, USA).

Morphometric analysis

A customized pipeline in Cell Profiler r10997 (Broad Institute, MIT) was written to calculate the pax 9 intensity of each cell and to count the number of DAPI-stained nuclei in each microarray spot. Cells were identified as primary objects based on their stained nuclei and cell bodies (labelled with GFP) were defined as the secondary objects; thresholds were was defined for both to respectively separate nuclei and labelled cell bodies from the background using the *Otsu Adaptive* algorithm. The range of diameters of nuclei was measured using ImageJ (NIH, Bethesda, Maryland); threshold bounds were set between 0.1 and 1.0 to rule out detection of background signals. The *Laplacian of Gaussian* method was found to give the best result when coupled with the *Intensity* module as a parameter to distinguish between clumped objects. From these identified objects, the total number of cells per spot and the average intensity of the Pax9 signal was measured and normalized against the varying level of cell adherence per condition. Cell densities were determined based on the total number of nuclei measured per spot, and the area of each spot (in um^2), which was quantified using ImageJ. The accuracy of the automated analysis was confirmed by manually measuring similar properties of cells adherent to microarray spots and quantifying using Image J software (NIH, Bethesda, Maryland).

Statistical Analysis

Statistical analyses were conducted using, one-way ANOVA for mechanical

characterization tests and two-way ANOVA with replication to compare the effects of ECM protein and substrate stiffness on cell adhesion and odontogenic differentiation. These were followed by tukey-post hoc tests. Results are presented as mean +/- standard error of the mean (SEM) unless otherwise stated.

Results and Discussion

Characterization of the ECM Microarrays

A microarray containing micrometer-sized, circular ECM islands (425 mm diameter) in a square array (spot-to-spot pitch of 900 mm) with defined mechanical and chemical properties was fabricated by microspotting ECM solutions on top of PAA gels that differ in their degree of cross-linking (Figure 4.1A). First, three square PAA gel pads (18 X 18 mm) of different ratios (1:0.1,1:0.25 and 1:1.25) of 40% acrylamide to 2% bisacrylamide were polymerized on a single microscope glass slide (Figure 4.1B), and ECM proteins were then spotted on top of the pads containing either collagen VI (100, 200 or 300 μg/ml) , tenascin (10 μg/ml), or a mixture of both. ECM proteins were diluted in buffer containing BSA to keep the concentration of protein constant (24 ug) in all combinations and to prevent protein polymerization as previously described [33].

When the mechanical properties of the PAA pads were quantified using rheometry, we found that gels created with the high, middle and low ratios of acrylamide to bisacrylamide exhibited elastic moduli of 132, 558 and 1510 Pa, respectively (Figure 4.2A).

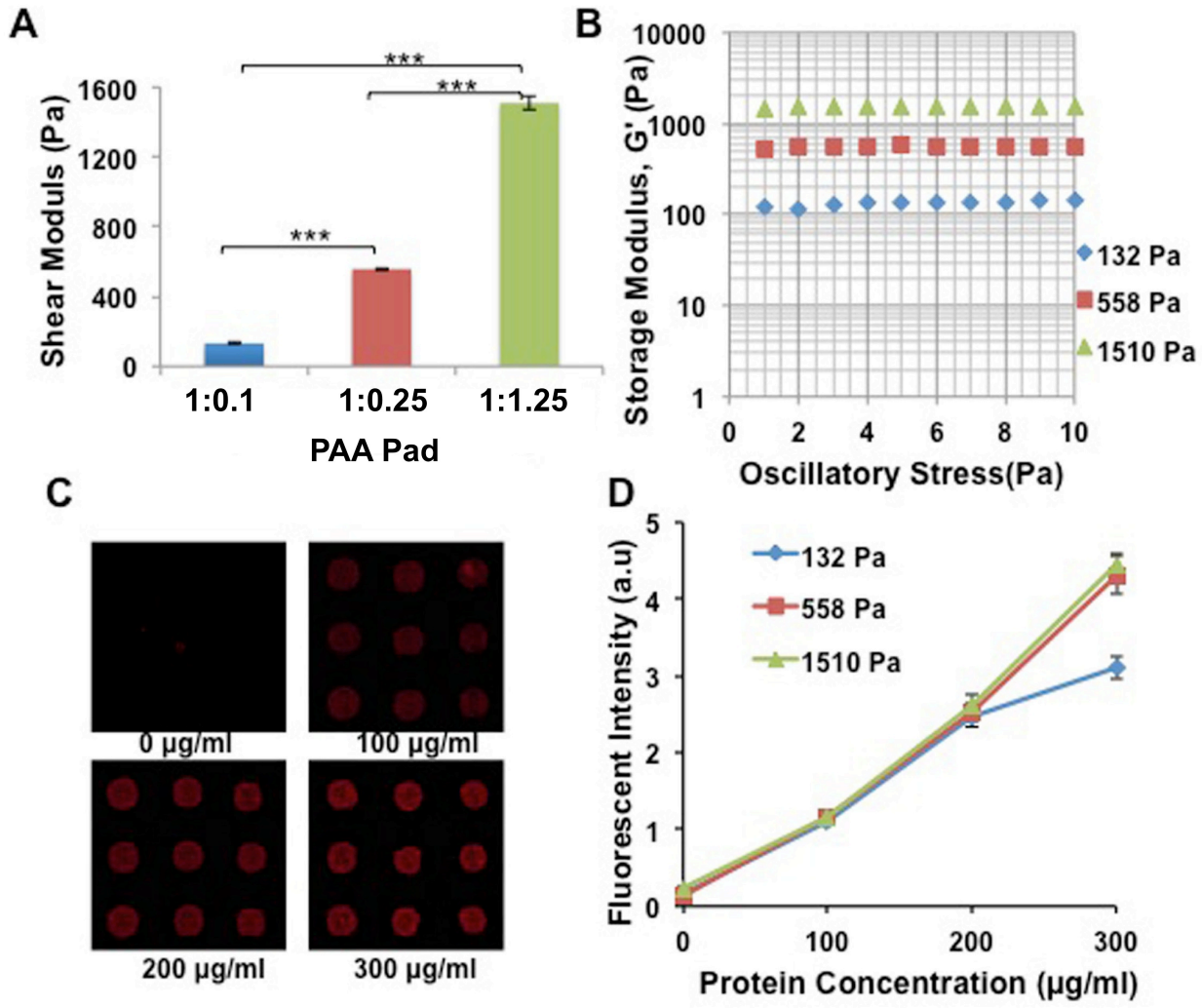

Figure 4.2 Microarray characterization. (A) Result of mechanical property characterization of three different PAA gel pads (***p<0.0001, Mean ± S.E.M.). (B) Stress dependence of G' for PAA gel pads. (B) Stress dependence of G' for PAA gel pads. (C) Microarray images of Rhodamine-labeled Fibronectin on 132 Pa PAA. (D) Fluorescent intensity (arbitrary units) measurements as a function of concentration.

The storage modulus (G') of each of the PAA gel pads also remained stable when the level of oscillatory stress was varied from 1 to 10 Pa (Figure 4.2B), which is critical to ensure the stability of the soft gels under printing conditions. We then

printed spots of rhodamine-labeled fibronectin to confirm our ability to spot ECM at defined concentrations on the PAA pads (Figure 4.1A). Fluorescence microscopic analysis of these printed substrates confirmed that the ECM proteins remained limited to precisely defined circular islands of approximately the same diameter that we printed (424 $\pm$ 51.8 μm), and that the fluorescent intensity increased in direct proportion to the concentration of fibronectin protein deposited on the PAA pad, regardless of its stiffness (Figure 4.2C,D).

Effects of ECM mechanics on cell size and density

To analyze the effects of these various substrate conditions on cell form and function, MM cells were plated on the slides, cultured overnight in serum-containing medium, and fixed one day later. Analysis of these substrates using fluorescence microscopy combined with computerized image analysis revealed that the cells attached only to the ECM protein spots (Figure 4.3).

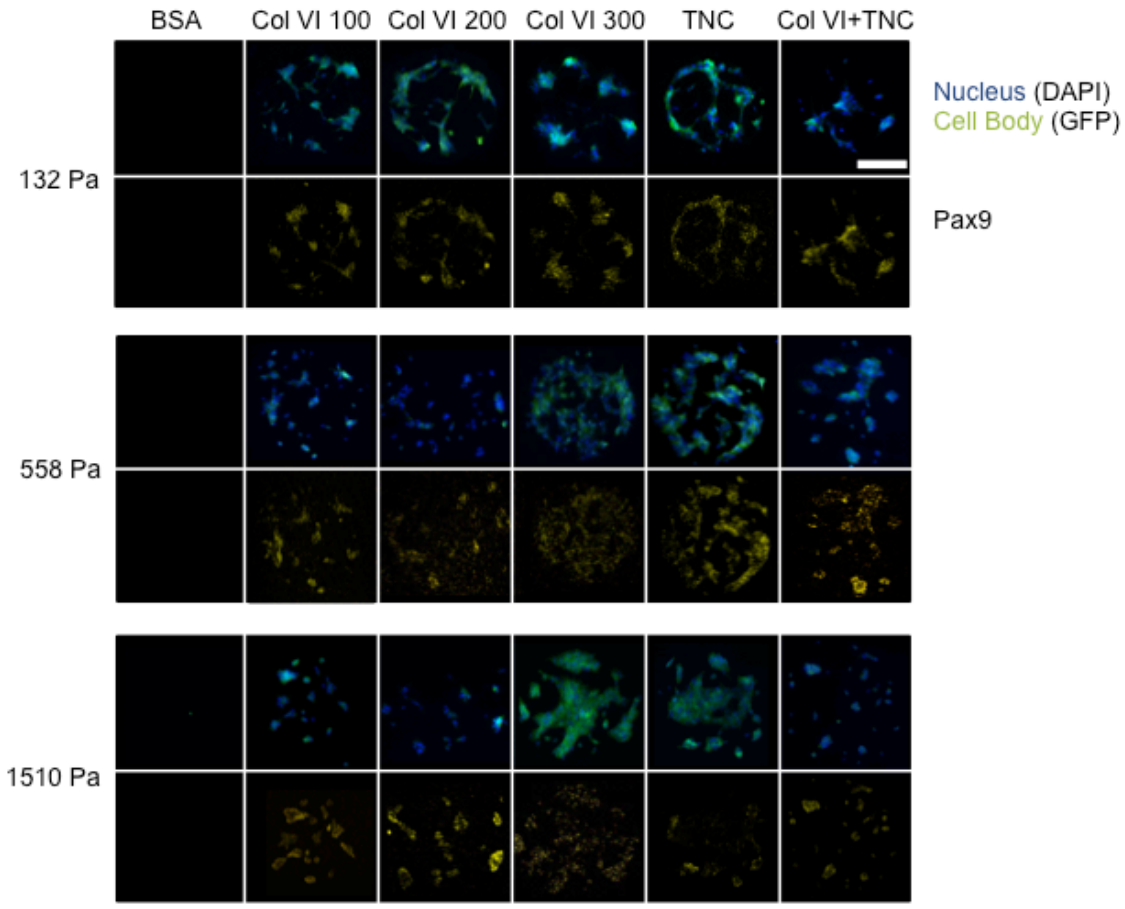

Figure 4.3 Micrograph images of microarrayed spots. Cells were cultured on the microarrayed ECM spots with 6 different protein conditions (BSA, Collagen VI 100, 200, and 300μg/ml, Tenascin 10 μg/ml and Tenascin-Collagen VI mixture printed on1510 Pa, 558 Pa, and 132 Pa PAA gel pads. 15 replicate spots/slide for each condition were printed and 4 microarray data sets were stained and analyzed. (Scale bar = 200 μm)

Similar results were obtained regardless of the stiffness of the PAA pad, and cells failed to adhere to control regions printed with the non-adhesive protein, BSA (Figure 4.3). Moreover, nearly identical adhesion responses were obtained in control studies in which cells were plated on ECM islands spotted on standard glass slides without

any PAA pads (Figure 4.4).

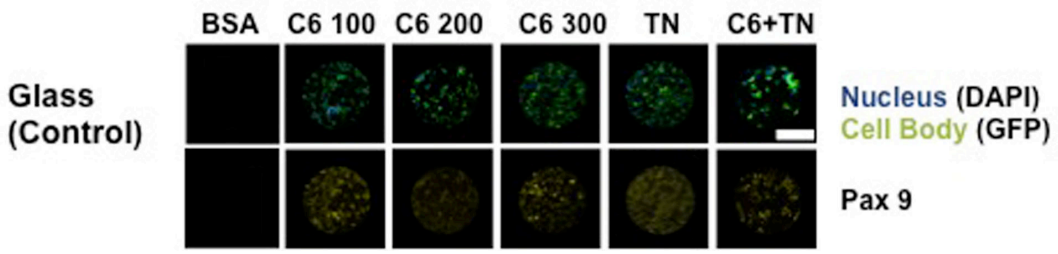

Figure 4.4. Immunofluorescent staining of control on glass surface treated with Collagen VI 100, 200, and 300 μg/ml, Tenascin 10 μg/ml, and Tenascin-Collagen VI mixture. (Scale bar = 200 μm)

A CellProfiler software pipeline was developed and used to outline nuclei and cells adherent to the imaged ECM spots (Figure 4.5), and to calculate the numbers of adherent cells as well as their mean projected cell areas.

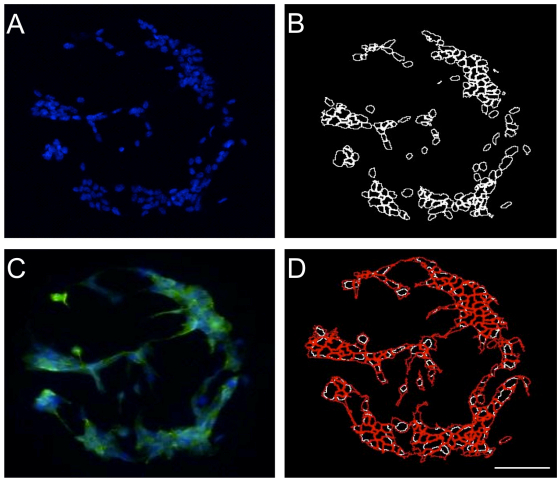

Figure 4.5 (A) Sample Input DAPI stained nuclei sample microarray spot inputted in CellProfiler. (B) Output image processed by CellProfiler identifying cell nuclei (white). (C) Sample microarray spot with DAPI stained nuclei and GFP labelled cell body. (D)

Figure 4.5 (Continued)…Output image processed by CellProfiler distinguishing cell body (red) from cell nuclei (white). (Scale bar = 200 μm).

Using this computerized image analysis to analyze cells adherent to spots with different ECM coating densities revealed that increasing collagen VI concentration from 100 to 300 μg/ml resulted in a corresponding rise in the density of cells adherent on each island (Figure 4.6A); however, the degree of this response varied depending on the stiffness of the PAA pad (Figure 4.6A).

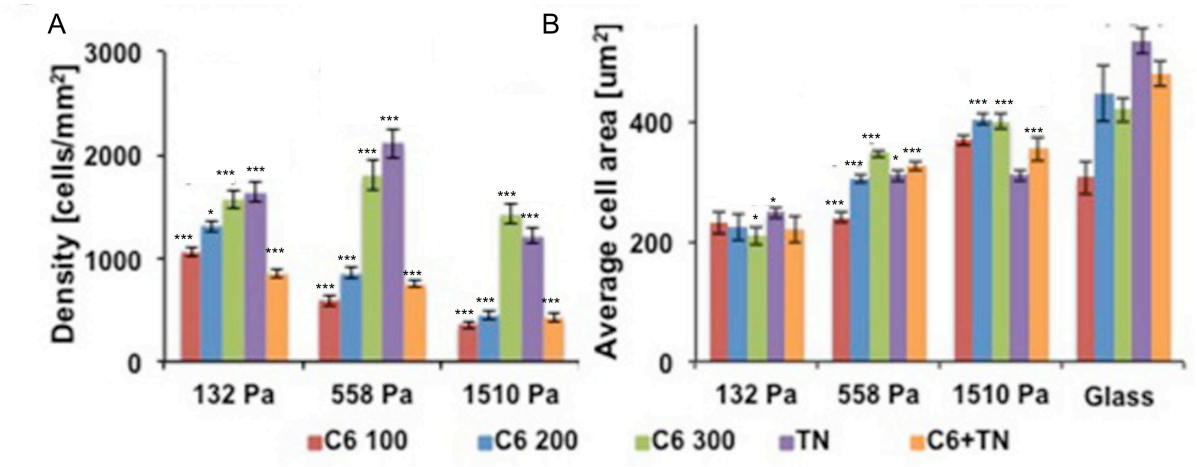

Figure 4.6 (A) Cell Density and (B) Cell Size as a function of varying PAA gel pad substrates and ECM proteins. (***p<0.0001, **p<0.001, *p<0.01, Mean ± S.E.M.)

Interestingly, tenascin and the highest collagen VI density (300 μg/ml) supported similar levels of cell adhesion, whereas printing them in combination on the same spot resulted in suppression of cell attachment to levels similar to those produced by 100 μg/ml collagen VI alone. This is consistent with past work showing that tenascin can inhibit integrin-dependent cell adhesion on substrates coated with other types of ECM molecules [34–36].

In contrast, cell spreading (projected cell area) was much less dependent on the chemical composition of the ECM spot, and more sensitive to the mechanics of the gel, with average cell areas increasing progressively as the stiffness of the substrate was raised (Figure 4.6B). Many previous reports have similarly shown that cell spreading increases as ECM substrate stiffness is raised [11,37,38]. In addition, cell extension was found to increase as the coating density of collagen VI was increased on rigid glass slides, as previous demonstrated with various other ECM proteins [39,40]. While a similar increase in spreading was observed when the coating concentrations of collagen VI were increased from 100 to 200 ug/ml on the moderate stiffness substrate, this was less evident on the stiffest substrate and it was completely lost on the most flexible PAA pad (Figure 4.6B). Interestingly, while the spots containing a mixture of collagen VI and tenascin were less effective at supporting cell adhesion than tenascin alone (Fig. 4.6A), the cells that adhered to these spots spread to similar degrees, although again spreading increased in direct proportion to the stiffness of the substrate (Fig. 4.6B).

ECM substrate-specific effects on tooth differentiation in MM cells

To determine whether this ECM microarray technology can be used to identify unique biomaterial properties that induce tissue-specific differentiation, we measured expression of the odontogenic transcription factor, Pax9, within embryonic MM cells and normalized against the varying level of adherence to the different combination described in Figure 6A. These studies revealed that, in general, cells exhibited the lowest levels of Pax9 expression on the intermediate stiffness (558 Pa) PAA pads regardless of the type or density of ECM coating, and the highest levels on the

stiffest (1510 Pa) PAA gel pads and rigid control glass substrates (Figure 4.7).

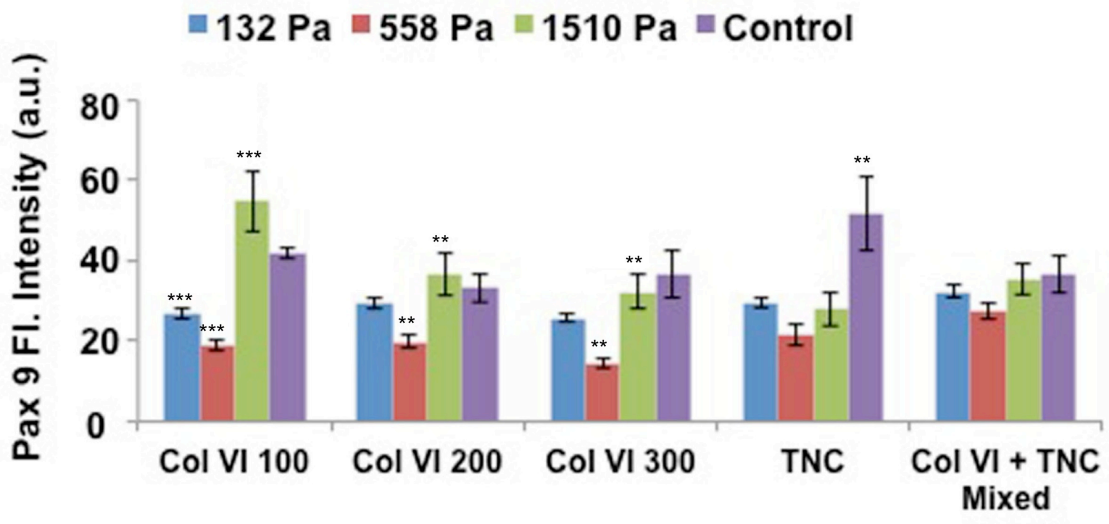

Figure 4.7 Pax 9 fluorescent Intensity (in arbitrary units) as a function of varying PAA gel pad substrates and ECM proteins. (***p<0.0001, **p<0.001, *p<0.01, Mean ± S.E.M.)

When we analyzed effects of varying ECM type, there was no detectable difference on the most flexible or intermediate (558 Pa) stiffness PAA pads. However, cells on the stiffest gels coated with the lowest collagen VI density (100 ug/ml) exhibited significantly higher levels of Pax9 expression than cells on higher coating densities. This raises the intriguing possibility that the particular *in vitro* mechanochemical features of this ECM spot more closely mimic the inductive tissue microenvironment that promotes tooth differentiation *in vivo*. Interestingly, tenascin had little effect on MM cell differentiation on any of the flexible substrates, whereas it was a potent inducer on a highly rigid glass substrate (Figure 4.7).

The methodology described in our study provides a unique and customized library that incorporates substrate stiffness in determining the inductive behavior of MM cells.

While the biomaterial library analyzed here was small compared to past high throughput screening technologies, our findings clearly demonstrate the concept and ease of developing a customized combinatorial microarray for determining the inductive capacity of very specific concentrations and combinations of certain ECM proteins on varying mechanical substrates with high flexibility. In addition, while we carried out our studies in 2D, there is currently a shift towards 3D printing technologies that more closely predict and recapitulate cell behavior and interactions [41,42]. Thus, it would be useful to extend this work to microarrays consisting of 3D gels of varying mechanical stiffness and coated with more ECM protein combinations in the future.

In summary, our study presents a novel microarray platform capable of analyzing the combinatorial effects of certain mechanical and chemical factors on cell density, spreading and induction of odontogenesis. To our knowledge, this is the first study to develop a microarray platform that can analyze combinatorial effects of ECM protein type, density and mechanics on embryonic cell differentiation. The information we generated using tooth differentiation as a model system also might be useful for the design of dental biomaterials that induce tooth formation in the future. In addition, this microarray system may be easily tuned to study combinatorial effects of mechanics and chemistry of other cell types of interest. Hence, it may be applied for a variety of tissue engineering studies that need to investigate the effects of mechanochemical microenvironmental cues on cell and tissue development *in vitro*.

Acknowledgements

This work was conducted with support by grants from NIH Common Fund (RL1DE019023 to D.E.I.) and the Wyss Institute for Biologically Inspired Engineering

at Harvard University. We would like to thank T. Mammoto for providing E10 MM cells.

References

[1] M.P. Lutolf, P.M. Gilbert, H.M. Blau, Designing materials to direct stem-cell fate., Nature. 462 (2009) 433–41. doi:10.1038/nature08602.

[2] C.J. Flaim, S. Chien, S.N. Bhatia, An extracellular matrix microarray for probing cellular differentiation, Nat. Methods. 2 (2005) 119–125. doi:10.1038/NMETH736.

[3] D.G. Anderson, S. Levenberg, R. Langer, Nanoliter-scale synthesis of arrayed biomaterials and application to human embryonic stem cells., Nat. Biotechnol. 22 (2004) 863–6. doi:10.1038/nbt981.

[4] A.J. Urquhart, D.G. Anderson, M. Taylor, A.R. Morgan, R. Langer, M.C. Davies, High Throughput Surface Characterisation of a Combinatorial Material Library, Adv. Mater. 19 (2007) 2486–2491. doi:10.1002/adma.200700949.

[5] S. Gobaa, S. Hoehnel, M. Roccio, A. Negro, S. Kobel, M.P. Lutolf, Artificial niche microarrays for probing single stem cell fate in high throughput, Nat. Methods. 8 (2011) 949–955. doi:10.1038/nmeth.1732.

[6] E.S. Place, N.D. Evans, M.M. Stevens, Complexity in biomaterials for tissue engineering., Nat. Mater. 8 (2009) 457–70. doi:10.1038/nmat2441.

[7] N. Huebsch, D.J. Mooney, Inspiration and application in the evolution of biomaterials, Nature. 462 (2009) 426–432. doi:10.1038/nature08601.

[8] T. Mammoto, A. Mammoto, D.E. Ingber, Mechanobiology and developmental control., Annu. Rev. Cell Dev. Biol. 29 (2013) 27–61. doi:10.1146/annurev-cellbio-101512-122340.

[9] T.R. Polte, G.S. Eichler, N. Wang, D.E. Ingber, Extracellular matrix controls myosin light chain phosphorylation and cell contractility through modulation of cell shape and cytoskeletal prestress., Am. J. Physiol. Cell Physiol. 286 (2004) C518–28. doi:10.1152/ajpcell.00280.2003.

[10] D.E. Discher, D.J. Mooney, P.W. Zandstra, Growth factors, matrices, and forces combine and control stem cells., Science. 324 (2009) 1673–7. doi:10.1126/science.1171643.

[11] A.J. Engler, S. Sen, H.L. Sweeney, D.E. Discher, Matrix Elasticity Directs Stem Cell Lineage Specification, Cell. 126 (2006) 677–689. doi:10.1016/j.cell.2006.06.044.

[12] C.S. Chen, M. Mrksich, S. Huang, G.M. Whitesides, D.E. Ingber, Geometric control of cell life and death., Science. 276 (1997) 1425–8.

[13] L.E. Dike, C.S. Chen, M. Mrksich, J. Tien, G.M. Whitesides, D.E. Ingber, Geometric control of switching between growth, apoptosis, and differentiation during angiogenesis using micropatterned substrates., In Vitro Cell. Dev. Biol. Anim. 35 (1999) 441–8. doi:10.1007/s11626-999-0050-4.

[14] R. Singhvi, A. Kumar, G.P. Lopez, G.N. Stephanopoulos, D.I.C. Wang, G.M. Whitesides, et al., Engineering Cell Shape and Function, Science (80-.). 264 (1994) 696–698.

[15] R.P. Hertzberg, A.J. Pope, High-throughput screening: new technology for the 21st century., Curr. Opin. Chem. Biol. 4 (2000) 445–51.

[16] C.A. Tweedie, D.G. Anderson, R. Langer, K.J. Van Vliet, Combinatorial Material Mechanics: High-Throughput Polymer Synthesis and Nanomechanical Screening, Adv. Mater. 17 (2005) 2599–2604. doi:10.1002/adma.200501142.

[17] F. Chowdhury, Y. Li, Y.-C. Poh, T. Yokohama-Tamaki, N. Wang, T.S. Tanaka, Soft substrates promote homogeneous self-renewal of embryonic stem cells via downregulating cell-matrix tractions., PLoS One. 5 (2010) e15655. doi:10.1371/journal.pone.0015655.

[18] N. Eroshenko, R. Ramachandran, V.K. Yadavalli, R.R. Rao, Effect of substrate stiffness on early human embryonic stem cell differentiation., J. Biol. Eng. 7 (2013) 7. doi:10.1186/1754-1611-7-7.

[19] M. Jaramillo, S.S. Singh, S. Velankar, P.N. Kumta, I. Banerjee, Inducing endoderm differentiation by modulating mechanical properties of soft substrates, J. Tissue Eng. Regen. Med. (2012). doi:10.1002/term.

[20] I. Levental, P.C. Georges, P. a. Janmey, Soft biological materials and their impact on cell function, Soft Matter. 3 (2007) 299. doi:10.1039/b610522j.

[21] T. Mammoto, A. Mammoto, Y. Torisawa, T. Tat, A. Gibbs, R. Derda, et al., Mechanochemical control of mesenchymal condensation and embryonic tooth organ formation., Dev. Cell. 21 (2011) 758–69. doi:10.1016/j.devcel.2011.07.006.

[22] B. Hashmi, L.D. Zarzar, T. Mammoto, A. Mammoto, A. Jiang, J. Aizenberg, et al., Developmentally-Inspired Shrink-Wrap Polymers for Mechanical Induction of Tissue Differentiation., Adv. Mater. (2014). doi:10.1002/adma.201304995.

[23] M. Mina, E. Kollar, The induction of odontogenesis in non-dental mesenchyme combined with early murine mandibular arch epithelium, Arch Oral Biol. 32 (1987) 123–127.

[24] R. Maas, M. Bei, The Genetic Control of Early Tooth Development, Crit. Rev. Oral Biol. Med. 8 (1997) 4–39. doi:10.1177/10454411970080010101.

[25] M. Horibe, T. Sawa, M. Kataoka, J.-I. Kido, T. Nagata, Regulation of tenascin expression in cultured rat dental pulp cells., Odontology. 92 (2004) 22–6. doi:10.1007/s10266-004-0038-1.

[26] I. Thesleff, E. Mackie, S. Vainio, R. Chiquet-Ehrismann, Changes in the distribution of tenascin during tooth development., Development. 101 (1987) 289–96.

[27] I. Thesleff, Epithelial-mesenchymal signalling regulating tooth morphogenesis, J. Cell Sci. 116 (2003) 1647–1648. doi:10.1242/jcs.00410.

[28] A. Fekonja, Hypodontia in orthodontically treated children, Eur. J. Orthod. 27 (2005) 457–60. doi:10.1093/ejo/cji027.

[29] W.A. Bolton, Disharmony in tooth size and its relation to the analysisand treatment of malocclusion, Angle Orthod. 28 (1958) 113–118.

[30] P. Holm-Pedersen, N.P. Lang, F. Müller, What are the longevities of teeth and oral implants?, Clin. Oral Implants Res. 18 (2007) 15–9. doi:10.1111/j.1600-0501.2007.01434.x.

[31] A. Mammoto, K.M. Connor, T. Mammoto, C.W. Yung, C.M. Aderman, G. Mostoslavsky, et al., A mechanosensitive transcriptional mechanism that controls angiogenesis, Nature. 457 (2009) 1103–1108. doi:10.1038/nature07765.A.

[32] R.J. Pelham, Y.-L. Wang, Cell locomotion and focal adhesions are regulated by, Proc. Natl. Acad. Sci. U. S. A. 94 (1997) 13661–13665.

[33] C.J. Flaim, S. Chien, S.N. Bhatia, An extracellular matrix microarray for probing cellular differentiation, Nat. Methods. 2 (2005) 119–125. doi:10.1038/NMETH736.

[34] C.R. Rüegg, R. Chiquet-Ehrismann, S.S. Alkan, Tenascin, an extracellular matrix protein, exerts immunomodulatory activities., Proc. Natl. Acad. Sci. U. S. A. 86 (1989) 7437–41.

[35] R. Chiquet-Ehrismann, P. Kalla, C.A. Pearson, K. Beck, M. Chiquet, Tenascin interferes with fibronectin action., Cell. 53 (1988) 383–390.

[36] R. Probstmeier, P. Pesheva, Tenascin-C inhibits beta1 integrin-dependent cell adhesion and neurite outgrowth on fibronectin by a disialoganglioside-mediated signaling mechanism., Glycobiology. 9 (1999) 101–14.

[37] T. Yeung, P.C. Georges, L.A. Flanagan, B. Marg, M. Ortiz, M. Funaki, et al., Effects of substrate stiffness on cell morphology, cytoskeletal structure, and adhesion., Cell Motil. Cytoskeleton. 60 (2005) 24–34. doi:10.1002/cm.20041.

[38] D.E. Discher, P. Janmey, Y.-L. Wang, Tissue cells feel and respond to the stiffness of their substrate., Science. 310 (2005) 1139–43. doi:10.1126/science.1116995.

[39] D.E. Ingber, J. Folkman, Mechanochemical switching between growth and differentiation during fibroblast growth factor-stimulated angiogenesis in vitro: role of extracellular matrix., J. Cell Biol. 109 (1989) 317–30.

[40] D. Mooney, L. Hansen, J. Vacanti, R. Langer, S. Farmer, D. Ingber, Switching from differentiation to growth in hepatocytes: control by extracellular matrix., J. Cell. Physiol. 151 (1992) 497–505. doi:10.1002/jcp.1041510308.

[41] D.B. Kolesky, R.L. Truby, A.S. Gladman, T.A. Busbee, K.A. Homan, J.A. Lewis, 3D Bioprinting of Vascularized, Heterogeneous Cell-Laden Tissue Constructs., Adv. Mater. (2014) 1–7. doi:10.1002/adma.201305506.

[42] A. Dolatshahi-Pirouz, M. Nikkhah, A.K. Gaharwar, B. Hashmi, E. Guermani, H. Aliabadi, et al., A combinatorial cell-laden gel microarray for inducing osteogenic differentiation of human mesenchymal stem cells., Sci. Rep. 4 (2014) 3896. doi:10.1038/srep03896.

Chapter 5: Conclusion

In this dissertation, I provided an in depth overview of organ regeneration from a developmental perspective, with a primary focus on tooth as a model organ system. I then described work I completed which provide proof-of-principle for engineering a synthetic tissue engineering scaffold inspired by the developmental induction mechanism that is employed during tooth development. Specifically, I was able to create scaffolds composed of thermosensitive polymers chemically modified with ECM adhesive ligands that support attachment of embryonic mesenchymal cells, and that induce a mesenchymal condensation-like compaction response when warmed to body temperature. Moreover, I was able to show that this mechanical actuation mechanism drives tooth differentiation in vitro and enhances formation of mineralized tooth tissues in vivo. In addition, I presented work I carried out that demonstrates the feasibility of adapting microarray spotting technology to screen for ECM scaffolds with appropriate combinations of mechanical and chemical properties that are best suited to induce tooth differentiation.

As described in Chapter 1, a century ago, much of developmental control was explained largely in mechanical terms, but this view lost favor once the molecular biology revolution emerged. However, there has been a great resurgence of interest in mechanobiology and developmental control, and recent insights into the key role that physical compression of mesenchymal cells plays during mesenchymal condensation-induced tooth formation served as the inspiration for my dissertation studies.

The key question I addressed is: can we develop artificial materials for tissue engineering that emulate a key embryological induction mechanism to artificially trigger

tissue differentiation and organ formation? This challenge was addressed by focusing on the recently uncovered mechanism by which physical condensation and compaction of embryonic dental mesenchyme cells triggers induction of genes that drive tooth differentiation. To mimic this process, I engineered a novel thermoresponsive hydrogel scaffold composed of poly(*N*-isopropylacrylamide) (PNIPAAm) chemically modified with a GRGDS cell attachment peptide, and showed that it induces compaction of mesenchymal cells grown within it when warmed close to body temperature. Shrinkage of this polymer scaffold in 3D at body temperature induced a decrease in size of cultured embryonic dental mesenchyme cells similar to that previously observed during mesenchymal condensation of this tissue in the embryo. This polymer shrinkage-induced cell size change also increased expression of genes encoding critical odontogenic transcription factors (e.g., Pax 9, Msx1) and morphogens (e.g., Bmp4) that drive tooth differentiation. In addition, implantation of these polymer scaffolds containing the dental mesenchymal cells under the kidney capsule of living mice resulted in increased neovascularization, as well as formation of both mineralized and calcified tooth tissues *in vivo.* Thus, this thermoresponsive polymer scaffold could indeed induce tissue differentiation by mimicking this developmentally-inspired mechanical actuation mechanism.

Past work has shown that inductive dental mesenchyme can form a whole tooth when recombined with embryonic or adult epithelium and implanted in an immune-protected site (under the kidney capsule) in mice [1–4]. Thus, one limitation of this study was that *in vivo* studies of the mesenchymal cell seeded polymer gel were conducted in the absence of epithelium. In the future, studies that incorporate

epithelium will be critical to determine the degree to which a fully differentiated tooth can form, and hence, to demonstrate the physiological (and potentially clinical) relevance of this approach.

Given the novelty of these findings and the polymer material engineered, plus its potential application for developmental engineering of a wide range of tissues that similarly depend on mesenchymal condensation for their induction in the embryo (e.g. salivary gland, pancreas, kidney, bone, and cartilage, etc) [5–8], these results may have broad relevance for the fields of tissue engineering and regenerative medicine, as well as developmental and stem cell biology. Although I only focused on RGD-polymerized scaffolds here and the role of soluble factors was not investigated, these parameters can be varied in the future to further optimize the tooth induction response and to tailor the scaffold for engineering of different organ types.

The microarray screening platform I described in Chapter 4 may be useful for identifying biomaterials with mechanical and chemical properties that are optimally supportive of tooth differentiation. This approach also can be extended to screen for biomaterials that regulate differentiation or other functions (e.g., growth) of any type of cell that similarly responds uniquely to different combinations of ECM chemical and mechanical properties.

The work I did on this microarray screening platform would have been greatly strengthened if I had the time to do an extensive ECM library analysis, and also simultaneously analyzed effects of combinations of many different soluble factors, which should be possible given the multiplexed nature of the systems I created. The testing platform also utilized a 2D approach that may not accurately depict the natural 3D tissue

microenvironment. Nevertheless, the microarray spotting method I described should facilitate and improve current materials screening methods and analyses.

While loss of teeth is not life-threatening, development of effective tooth engineering methods may be useful for treating conditions, such as hypodontia, in which teeth fail to form. This is a particularly significant problem in children because teeth implants cannot be used due to the dynamic growth properties of the child's jaw. However, the same design principles we leveraged to fabricate synthetic materials that promote tooth differentiation are also used to induce formation of many other organs. This mechanically-actuable scaffolds for tissue engineering I described here may therefore also be applied to studies with more complex organs in the future. But to me, the greatest significance of this work is that it opens a new avenue of exploration in the field of tissue engineering by demonstrating the feasibility of designing, fabricating and experimentally validating 'developmentally-inspired' biomaterials.

References:

[1] Mammoto T, Mammoto A, Torisawa Y, Tat T, Gibbs A, Derda R, et al. Mechanochemical control of mesenchymal condensation and embryonic tooth organ formation. Dev Cell 2011;21:758–69.

[2] Oshima M, Mizuno M, Imamura A, Ogawa M, Yasukawa M, Yamazaki H, et al. Functional tooth regeneration using a bioengineered tooth unit as a mature organ replacement regenerative therapy. PLoS One 2011;6:e21531.

[3] Ohazama A, Modino SAC, Miletich I, Sharpe PT. Stem-cell-based tissue engineering of murine teeth. J Dent Res 2004;83:518–22.

[4] Nakao K, Morita R, Saji Y, Ishida K, Tomita Y, Ogawa M, et al. The development of a bioengineered organ germ method. Nat Methods 2007;4:227–30.

[5] Smith MM, Hall BK. Development and evolutionary origins of vertebrate skeletogenic and odontogenic tissues. Biol Rev Camb Philos Soc 1990;65:277–373.

[6] Hall BK, Miyake T. Divide, accumulate, differentiate: cell condensation in skeletal development revisited. Int J Dev Biol 1995;39:881–93.

[7] Hall BK, Miyake T. The membranous skeleton : the role of cell condensations in vertebrate skeletogenesis. Anat Embryol (Berl) 1992;186:107–24.

[8] Hall BK, Miyake T. All for one and one for all: condensations and the initiation of skeletal development. Bioessays 2000;22:138–47.

Supplementary Figures and Videos

Hashmi B, Zarzar L, Mammoto T, Mammoto A, Jiang A, Aizenberg J, and Ingber DE. Developmentally-Inspired Shrink-Wrap Polymers for Induction of Tissue Differentiation. *Adv. Materials* 2014; Feb 18 [Epub ahead of print].

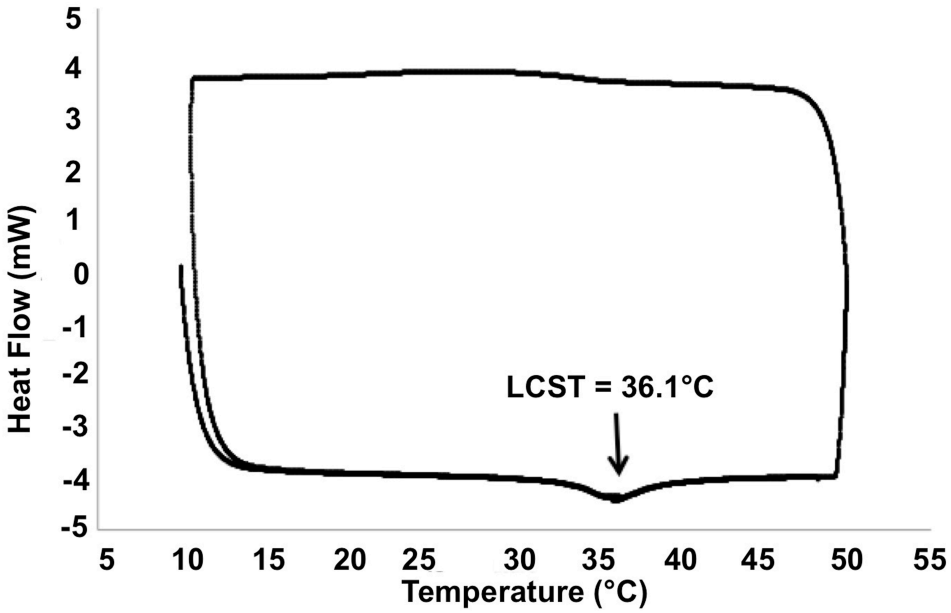

Figure S1 Graph of a Differential Scanning Calorimetry plot for a representative GRGDS-PNIPAAm gel indicating the LCST of this material to be ~ 36°C.

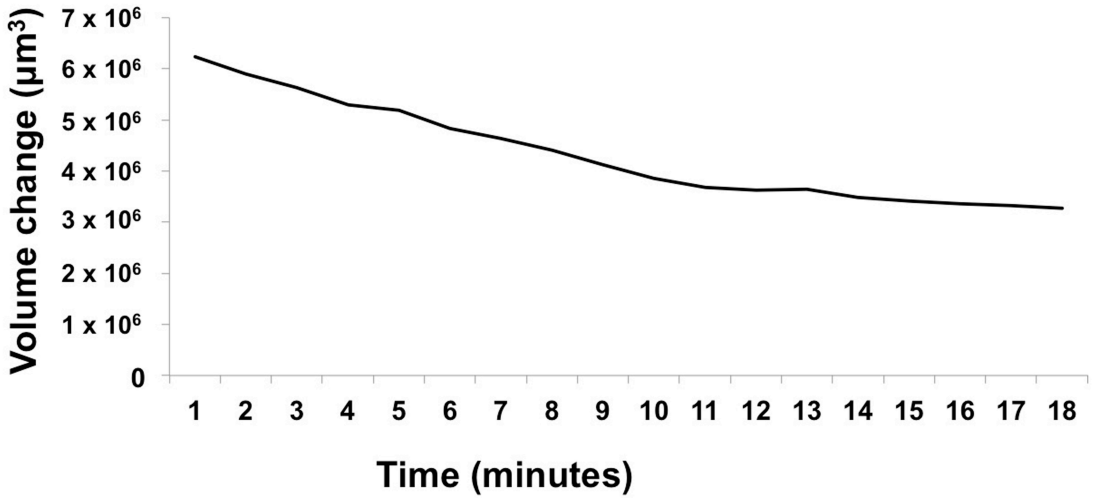

Figure S2 Dental mesenchymal (DM) cell volume change in a GRGDS-PNIPAAM gel when induced to contract by heating from ~30-40°C. Gel contraction initiated soon after the temperature was raised above the 36°C transition temperature and it reached completion within 10-15 min, as shown in Supplementary Video 1.

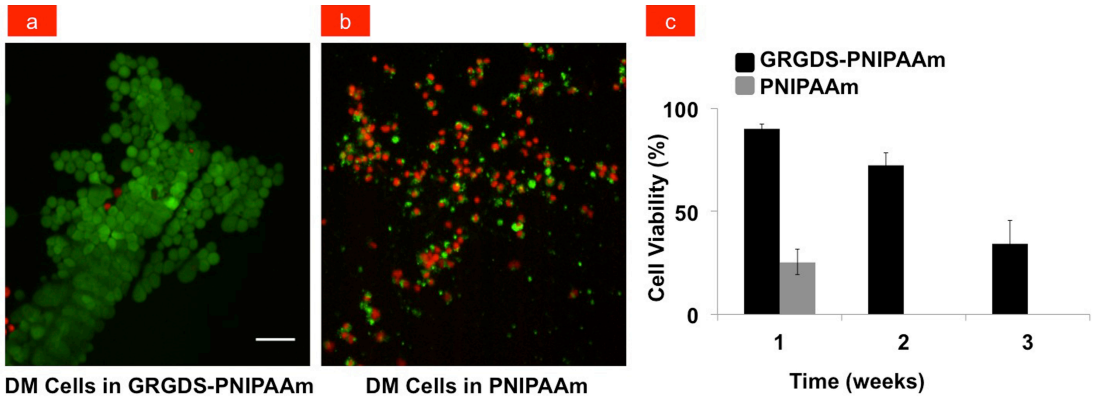

Figure S3 Biocompatibility of GRGDS-PNIPAAm gels. (a) Live (green) and dead dental mesenchymal (DM) cells (red) in a contracted GRGDS-PNIPAAm hydrogel after one week. (b) Live (green) and dead cells (red) in PNIPAAm hydrogel of the same formulation but without GRGDS peptide after one week (scale bar, 50 µm). (c) Graph showing quantification of cell viability in GRGDS-PNIPAAm hydrogels (black bars) and PNIPAAm hydrogels (grey bars); mean ± SEM.

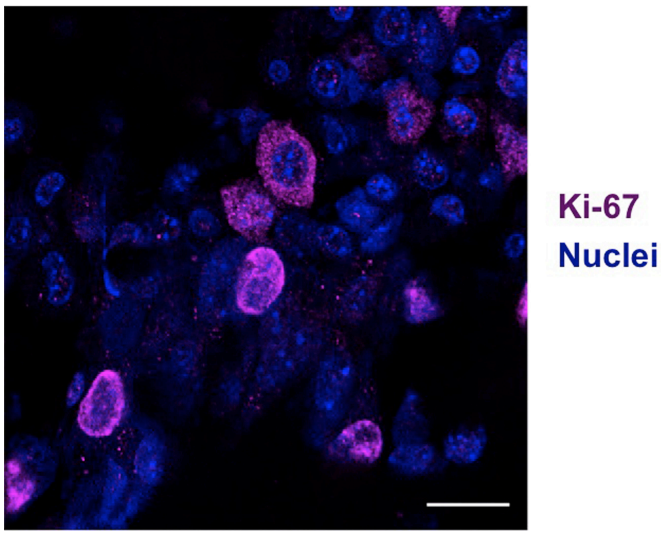

Figure S4 Fluorescent micrographs showing Ki-67 protein expression (magenta) in DAPI-labeled nuclei (blue) of dental mesenchymal (DM) cells cultured in a contracted GRGDS-PNIPAAm gels for 3 days (bar, 20 μm).

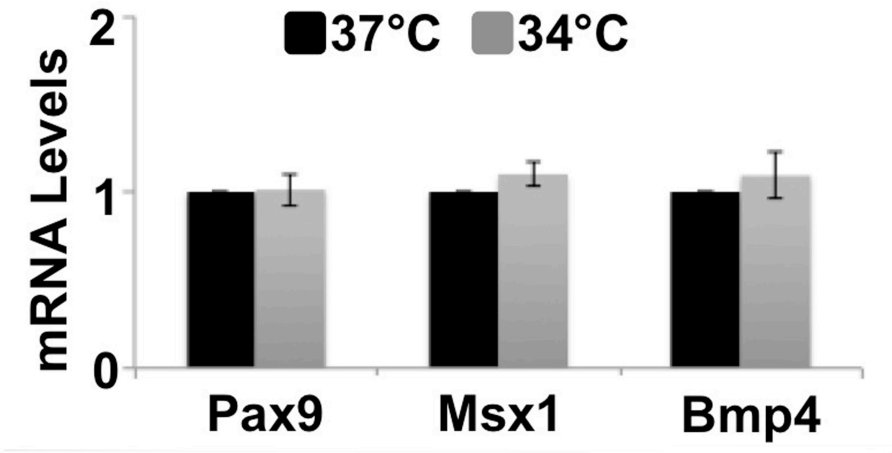

Figure S5 mRNA expression of Pax9, Msx1, and Bmp4 in dental mesenchymal cells cultured in 37°C (black bars) and 34°C (grey bars) for 76 hours indicating that temperature difference alone does not significantly influence expression.

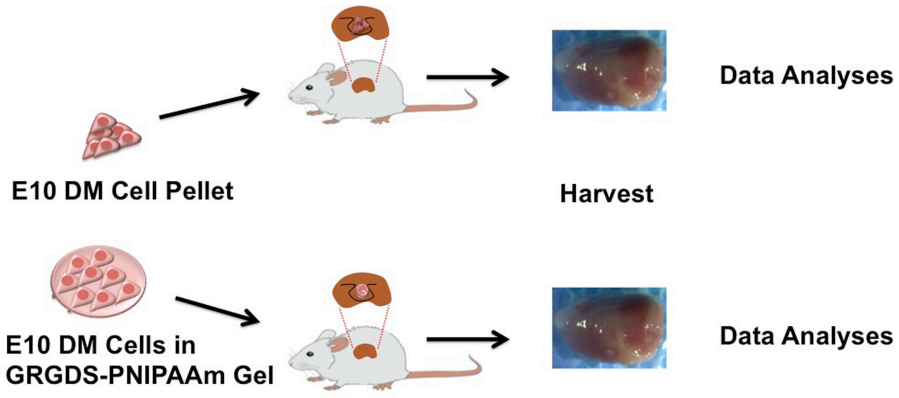

Figure S6 Representative diagram of experimental protocol for the *in vivo* studies.

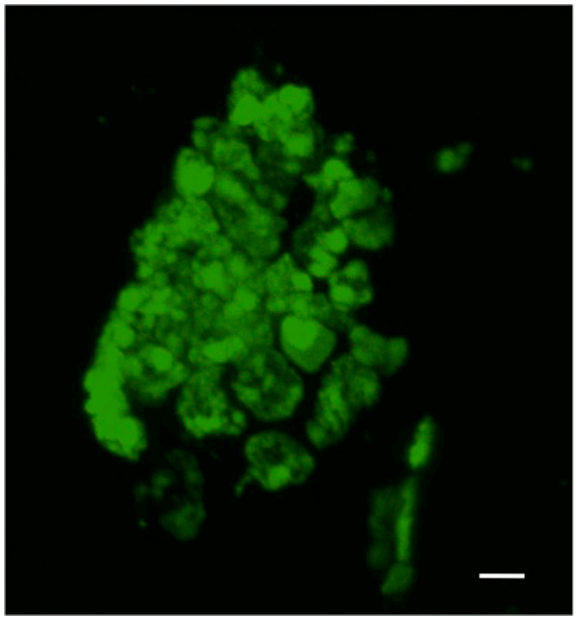

Figure S7 Compacted GFP-labelled DM cells seeded in a contracting GRGDS-PNIPAAm gel implanted 2 weeks *in vivo* (bar, 20 μm).

Video 1 A 2D time-lapse recording showing the GRGDS-PNIPAAm gel response to temperature change (from ~30°C-40°C). The gel rapidly begins to contract once the chamber temperature reaches the gel's LCST of ~36°C, and it completes this response within about 15 min.

Video 2 3D time-lapse recording of GFP-labelled DM cells (green) within the same gel from Video 1 in response to the same temperature change. Once the chamber temperature reaches the gel's LCST, the DM cells immediately compact due to the shrinkage of the gel pores, as shown in Figure 3.1c.